SKA脉冲星科学专题研讨会暨第十二届全国脉冲星年会

The progenitors of accretion-induced collapse events and the formation of particular NS systems

Liu Dongdong (刘栋栋)

Yunnan Observatories, CAS

Henan·Nanyang　　2023.7.3

Outline

- Backgroud of accretion-induced collapse (AIC) events
- Progenitor models of AIC events
  - (1) The ONe WD+RGB channel
  - (2) The ONe WD+He star channel
  - (3) The Double WD merger model
  - (4) The ONe WD+He WD channel
- Summary

Backgrounds

✓The AIC process has been proposed decades ago.

✓Massive ONe WDs, electronic capture supernovae, collapse to NSs

NSs peaked around 1.25M$_\odot$ originate from the AIC processes

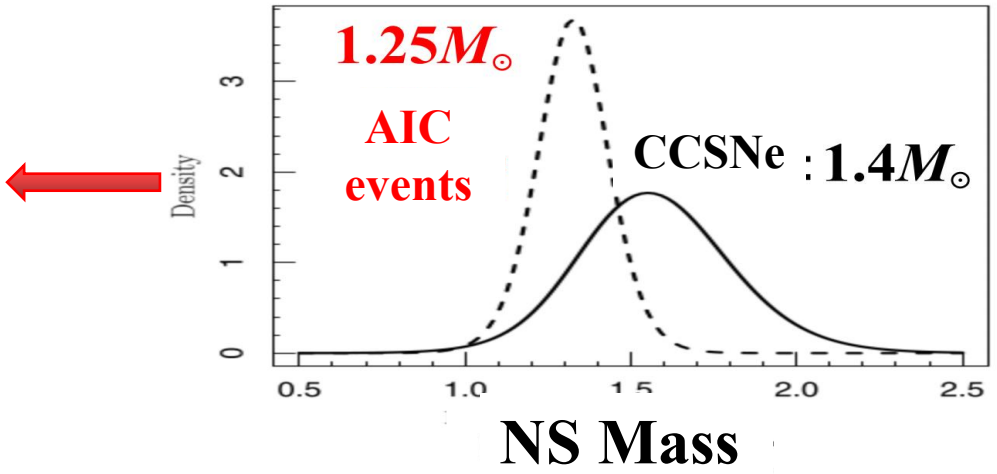

✓The AIC process can produce some important objects:

(1) Millisecond pulsars

(2) Intermediate-/low-mass binary pulsars

(3) Gravitational wave sources ……

Progenitor models

1. The single-degenerate model:

ONe WD + MS

ONe WD + RG

ONe WD + He star

2. The double-degenerate model:

ONe WD + ONe/CO WD

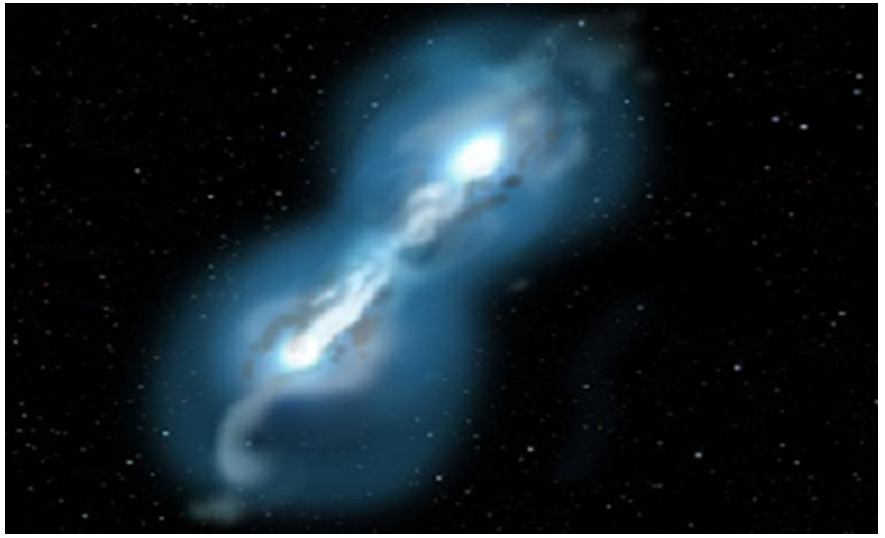

Progenitor models

1. The single-degenerate model:

ONe WD + MS

ONe WD + RG

ONe WD + He star

2. The double-degenerate model:

ONe WD + ONe/CO WD

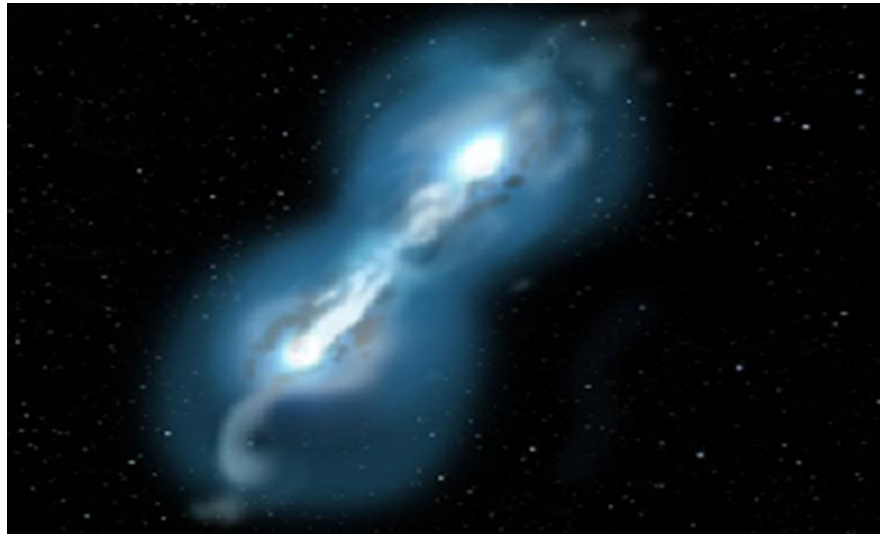

Millisecond pulsars with long orbital periods

- ✓The formation of MSPs with long orbital period (50-500 day) is unclear
- ✓Binary system will be disrupted during normal supernova explosion
- ✓Evolving ONe WD+RG systems to NS+RG systems via the AIC processes
- ✓Eventually form MSP+He WD systems with long orbital periods

Wang, Liu & Chen 2022, MNRAS

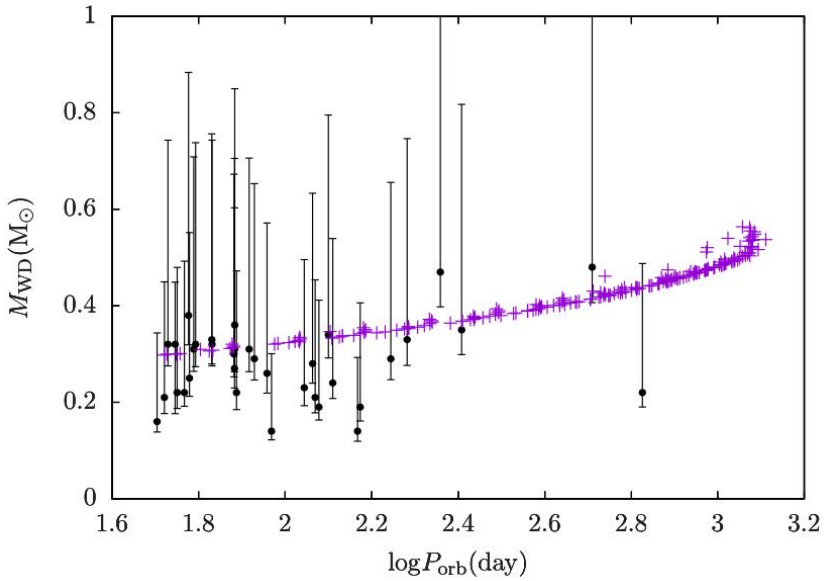

Progenitor models

1. The single-degenerate model:

ONe WD + MS

ONe WD + RG

ONe WD + He star

2. The double-degenerate model:

ONe WD + ONe/CO WD

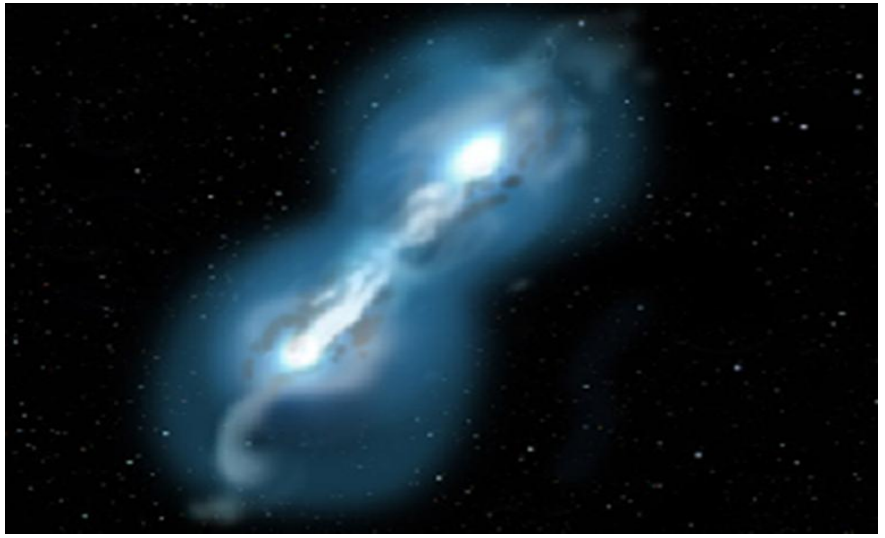

Intermediate-mass binary pulsars

✓**Intermediate-mass binary pulsars：**

long spin periods (10-200 ms);

$M_{WD} > 0.4\ M_{\odot}$

✓**Millisecond pulsars：**

short spin periods (1-30 ms);

$0.15\ M_{\odot} < M_{WD} < 0.4\ M_{\odot}$

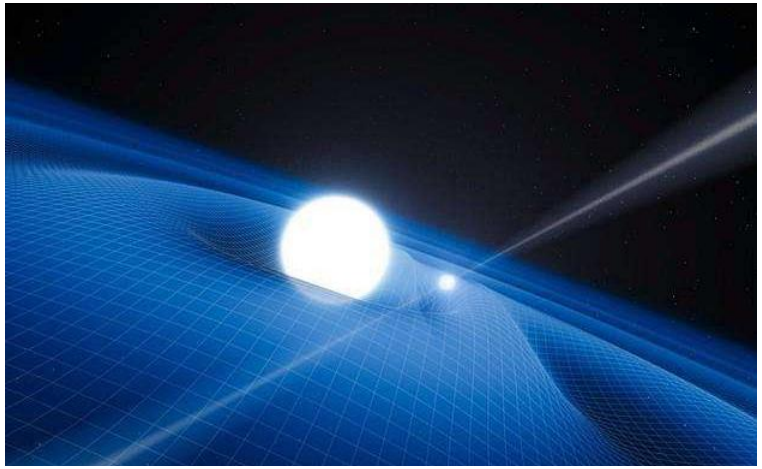

WD + Pulsar

The formation channel of intermediate-mass binary pulsars

✓**intermediate-mass X-ray binary channel**

NS+MS （2.0—10 $M_{\odot}$）

IMBPs with orbital periods ~ 3-50 d

(van den Heuvel 1975； Tauris et al. 2000)

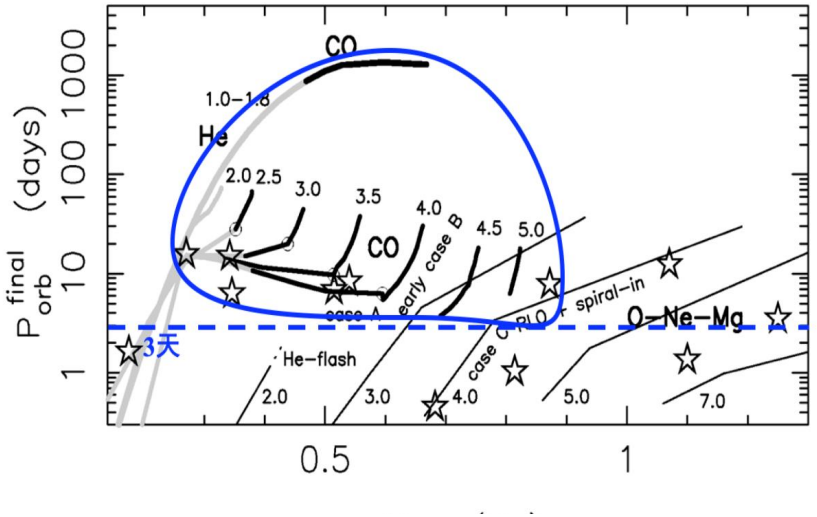

✓**NS+He star channel：**

Part of IMBPs with orbital periods < 3 d

(Chen & Liu 2013)

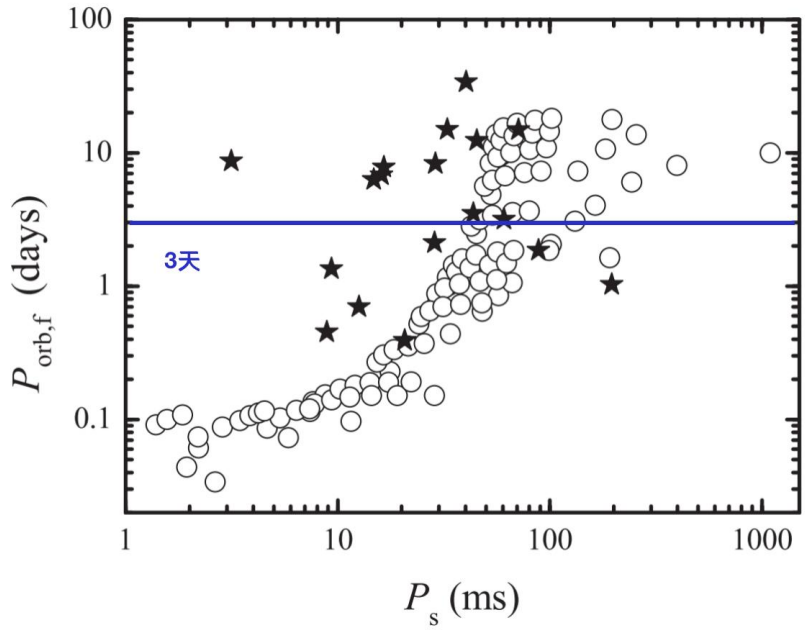

The formation channel of intermediate-mass binary pulsars

✓**intermediate-mass X-ray binary channel**：

NS + 2.0—10 $M_{\odot}$ MS (van den Heuvel 1975)

IMBPs with orbital periods ~ 3-50 d (Tauris et al. 2000)

✓**NS+He star channel**：

Part of IMBPs with orbital periods < 3 d (Chen & Liu 2013)

✓**The AIC channel of ONe WD+He star systems**：

Explained the formation of IMBPs with short Obital periods

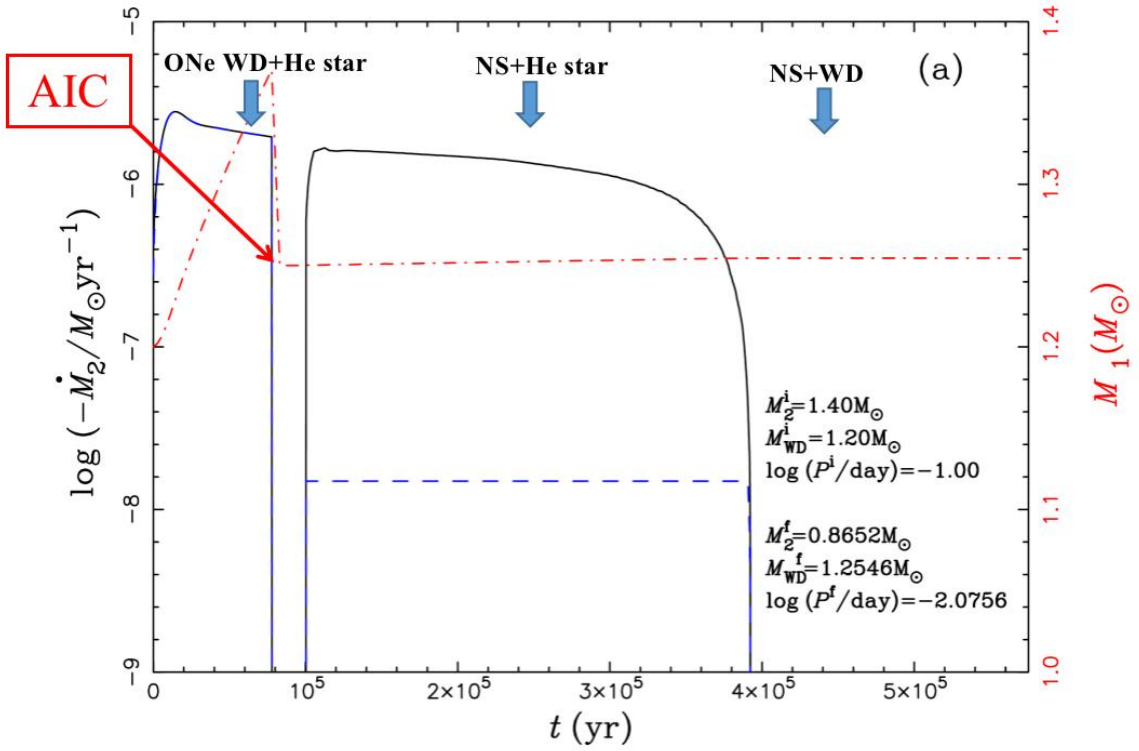

Binary evolution example

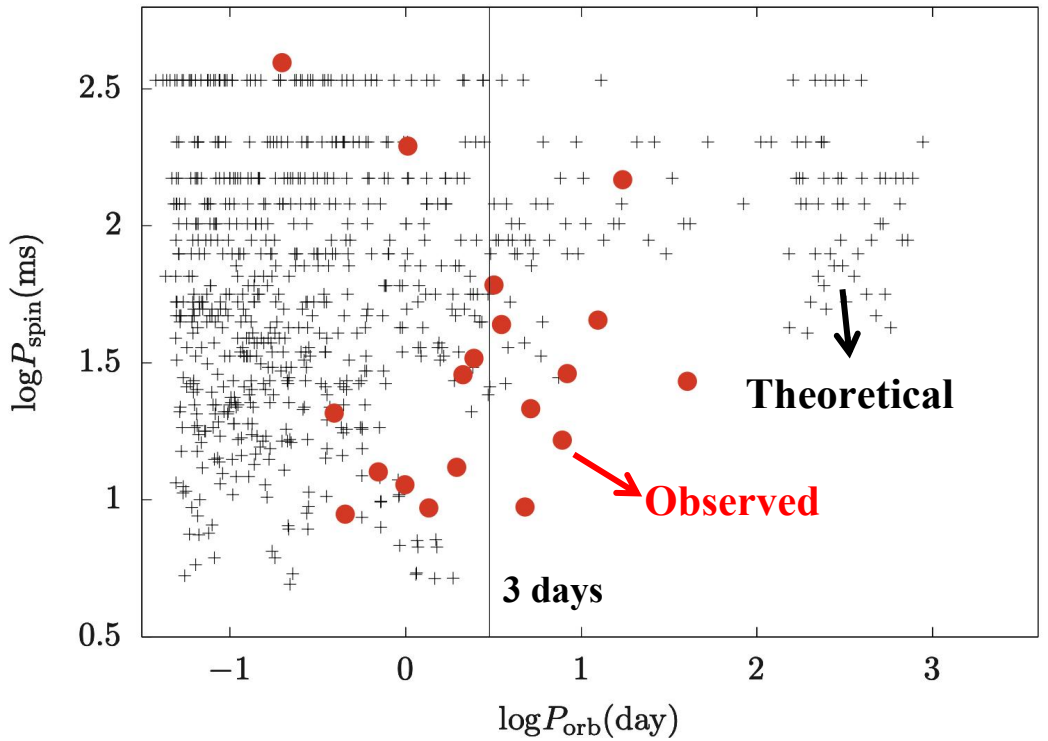

Comprison with observations

Reproducing the evolutionary history of PSR J0621+1002

Observed values:

- M_{NS}=1.24±0.11 $M_\odot$
- M_{WD}=0.78±0.04 $M_\odot$
- log(P_{orb})= - 0.1549
- P_{spin}=12.6 ms

Modeled values:

- M_{NS}=1.2583 $M_\odot$
- M_{WD}=0.8079 $M_\odot$
- log(P_{orb})= - 0.1549
- P_{spin}≈12 ms

Faulkner et al. (2004)

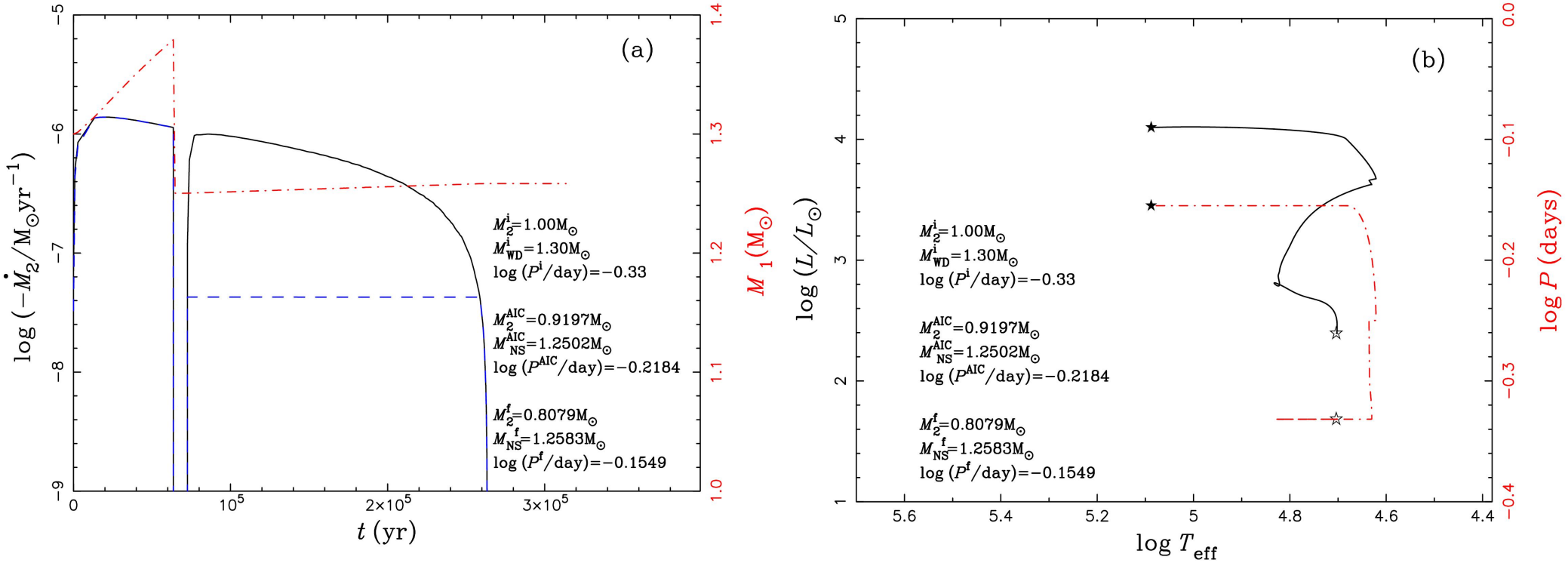

Progenitor models

1. The single-degenerate model:

ONe WD + MS

ONe WD + RG

ONe WD + He star

2. The double-degenerate model:

ONe WD + ONe/CO WD

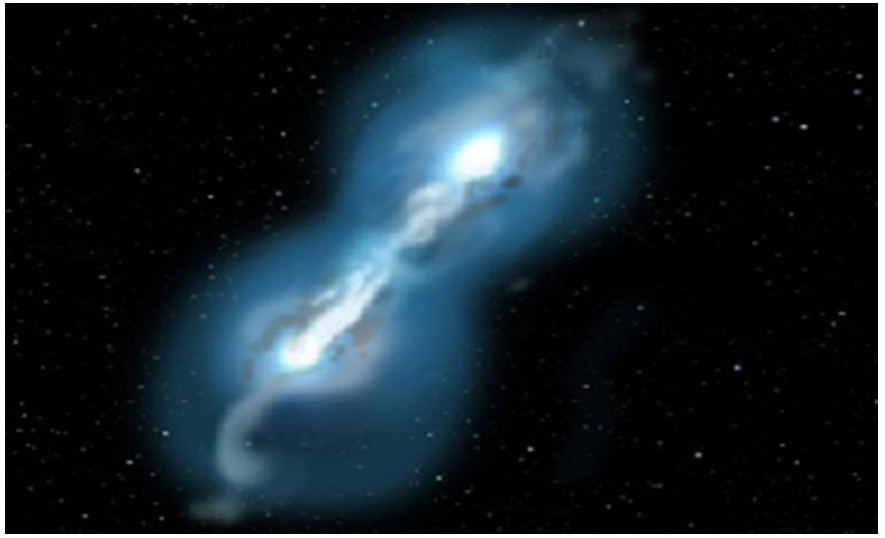

Double WD mergers will evolve to isolated NSs

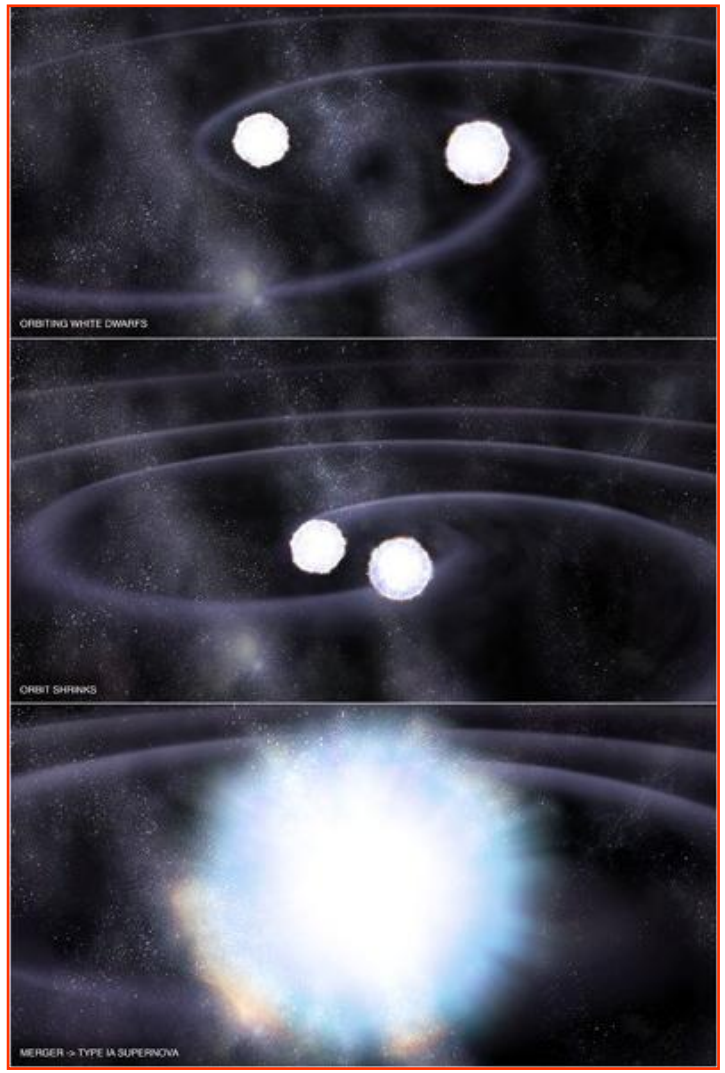

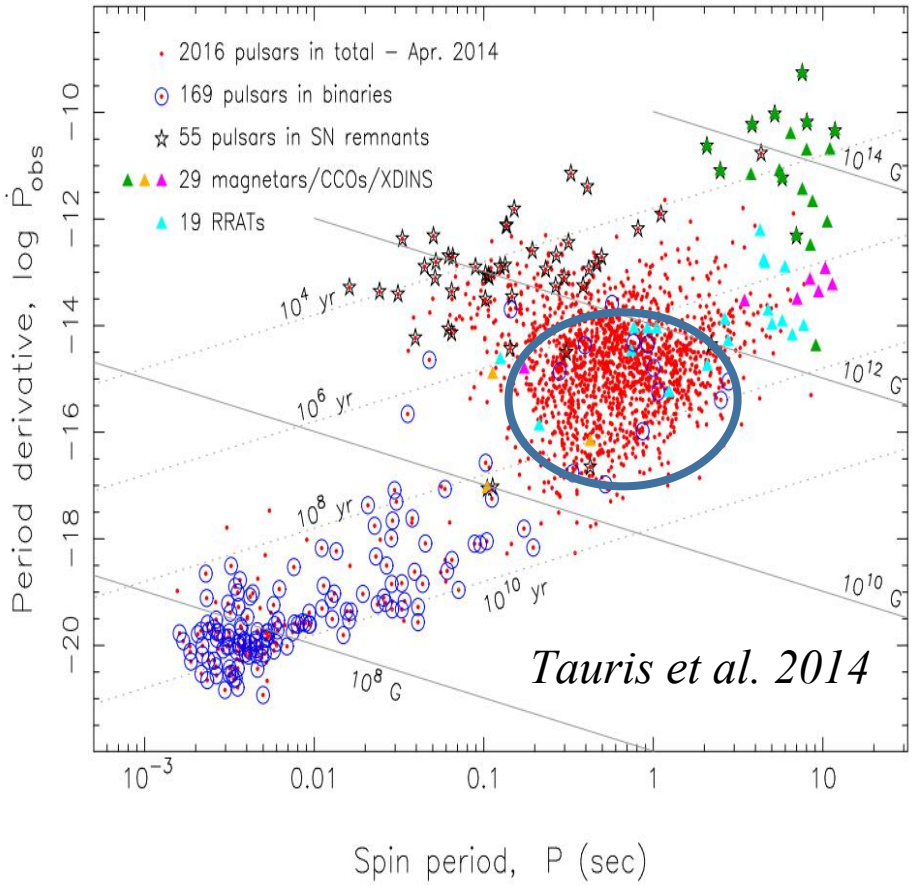

Galactic AIC birthrate and isolated NS number

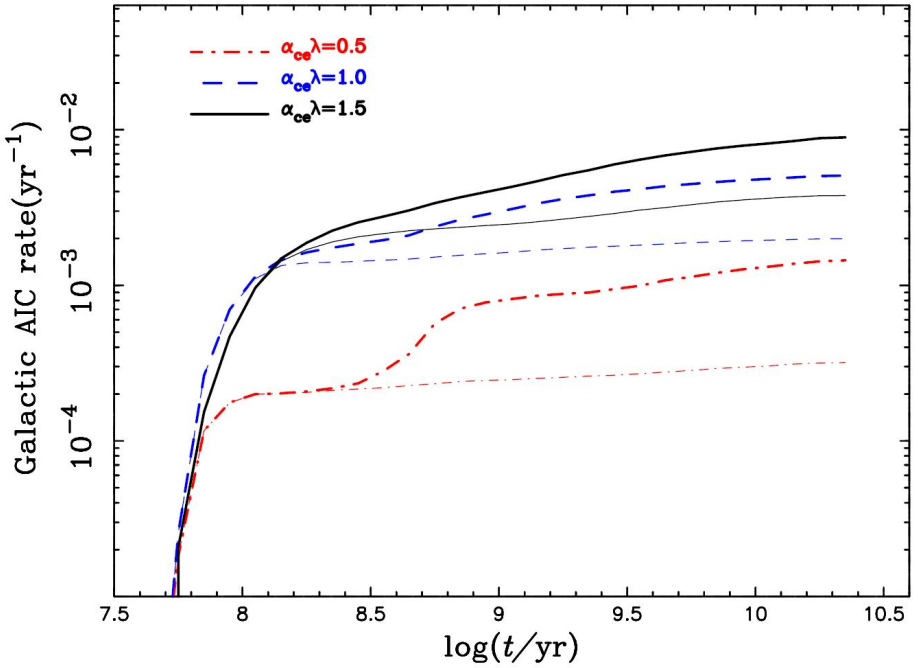

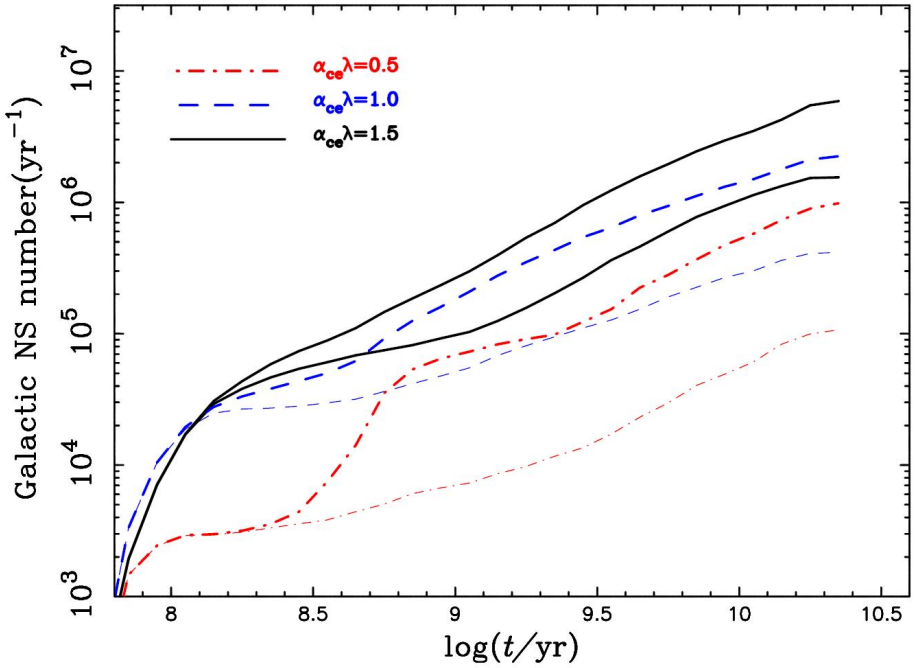

Birthrates of AIC supernoave：
1—10/1000 yr

NS number：10^5—6*10^6

Liu & Wang, 2020, MNRAS, 494, 3422

利用LAMOST数据，发现了一个吸积致塌缩事件前身星候选体：

LAN 11是一个ONe WD+sdB系统，将通过双简并星通道形成吸积致塌缩事件

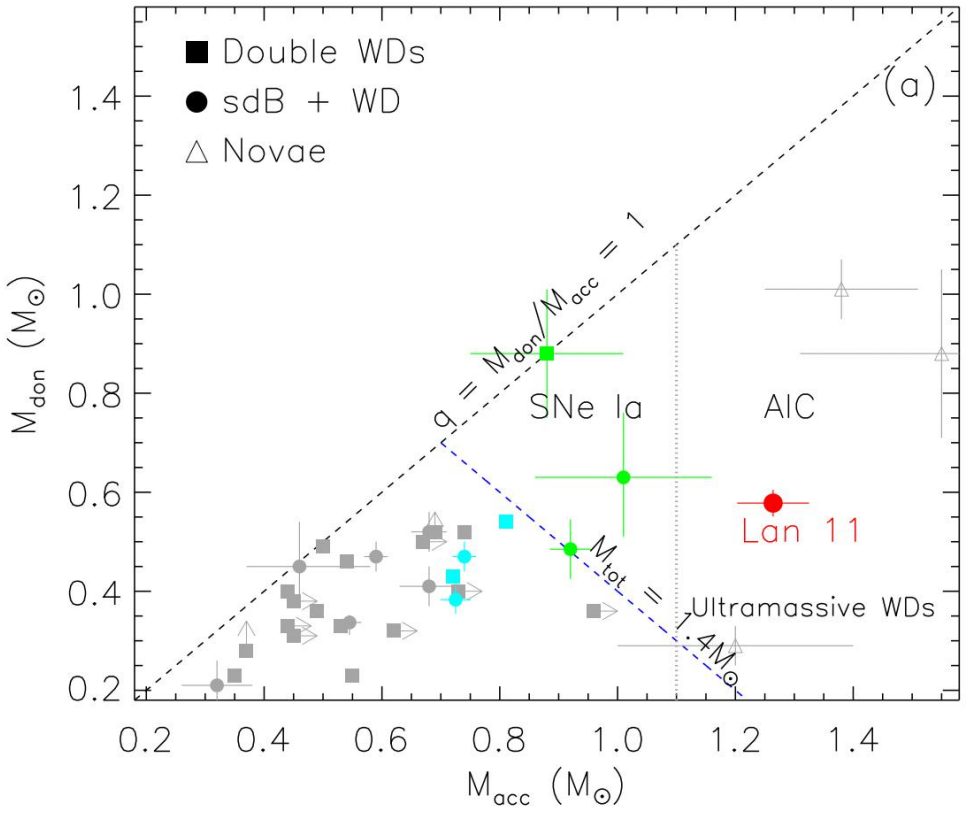

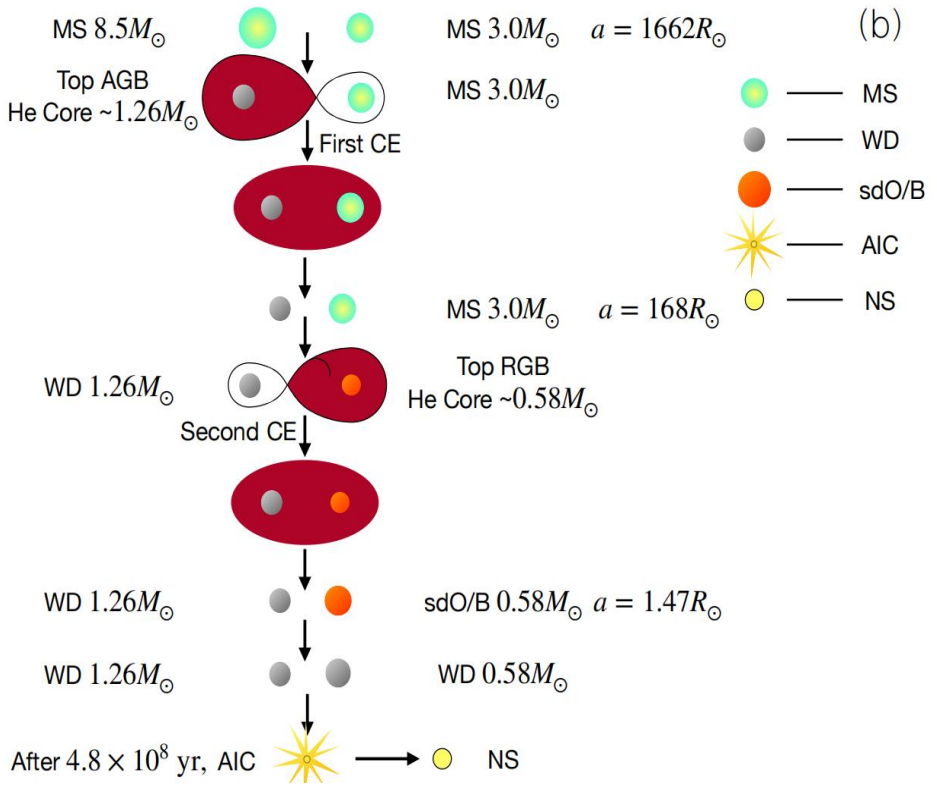

与刘超研究团队、刘继峰研究团队合作完成

ONe WD+He star系统通过双白矮星并合形成AIC的初始参数空间

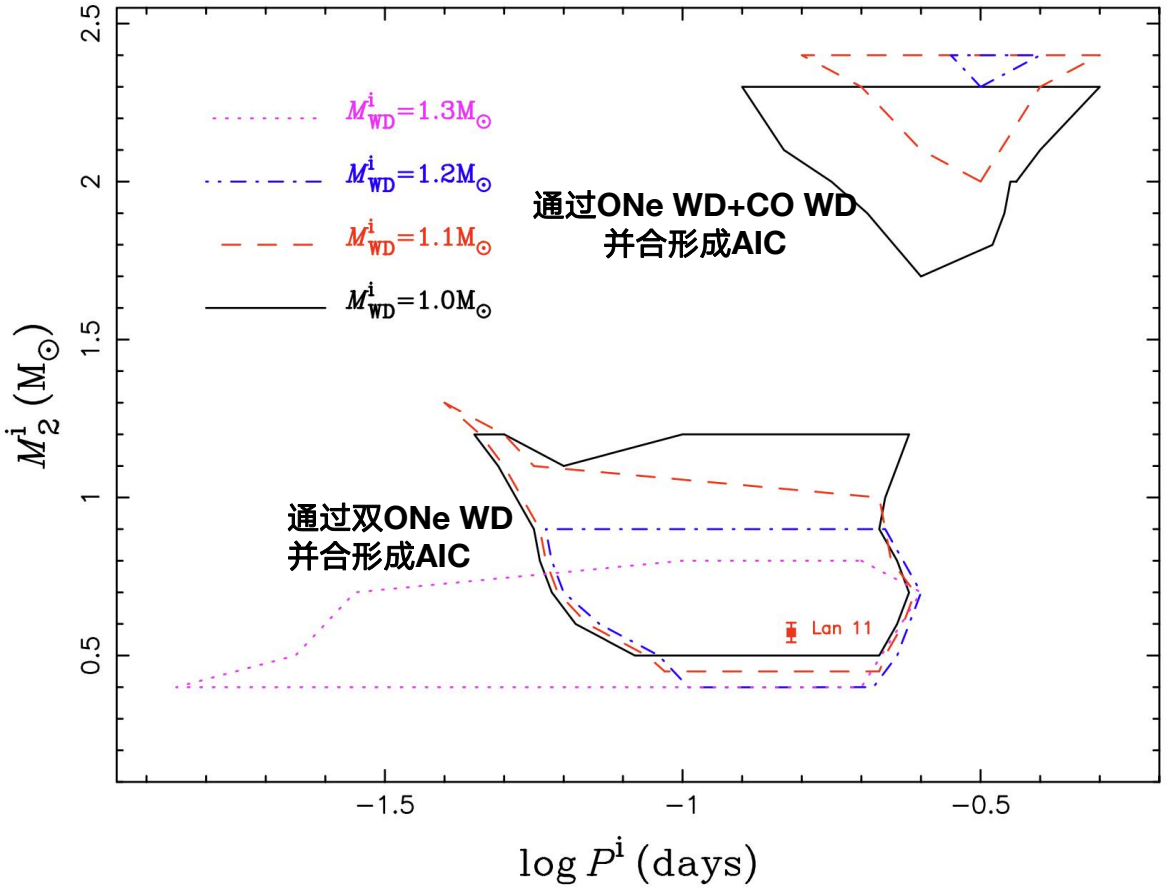

Llu & Wang 2020, MNRAS

Still no direct observed evidence for AIC events

✓**Very hard to detect：**

(Woosley& Baron 92; Piro & Kulkarni 13; Dessart+16; Brooks+18)。

Ejected mass < 0.1 $M_\odot$

^{56}Ni production < 0.01 $M_\odot$

5 magnitude fainter than a typical SN Ia

Last for only a few days

✓**There are many indirect evidence ……**

Evidence for AIC in globular clusters

- Small mass and small kick velocity of AIC:

  (1) The low space velocities of many recycled pulsars;

  (2) The large fraction of NSs retained in globular clusters.

  Bailyn & Grindlay (1990)

- The newly formed NSs with small kicks from the AIC channel:

  The detection of apparently young NSs in globular clusters.

  Lyne et al. (1996); Boyles et al. (2011)

Evidence for AIC in Galactic disk

Name	P (ms)	B (G)	Porb (days)	Mcomp ($M_\odot$)	Ref.
GRO J1744-28	467	$1.0*10^{13}$	11.8	~0.08	Van Paradijs+(1997)
PSR J1744-3922	172	$5.0*10^{9}$	0.191	~0.1	Breton+ (2007)
PSR B1831-00	521	$2.0*10^{10}$	1.81	~0.08	Sutantyo & Li (2000)
4U 1626-67	7680	$3.0*10^{12}$	0.028	~0.02	Yungelson+ (2002)

- NSs with slow spin and relatively high B field
- Ultra-light (semi)degenerate companion stars (<0.1 $M_\odot$)
- Close orbit

- NSs with slow spin and relatively high B field:

  Newly formed NSsHave not experienced mass-a

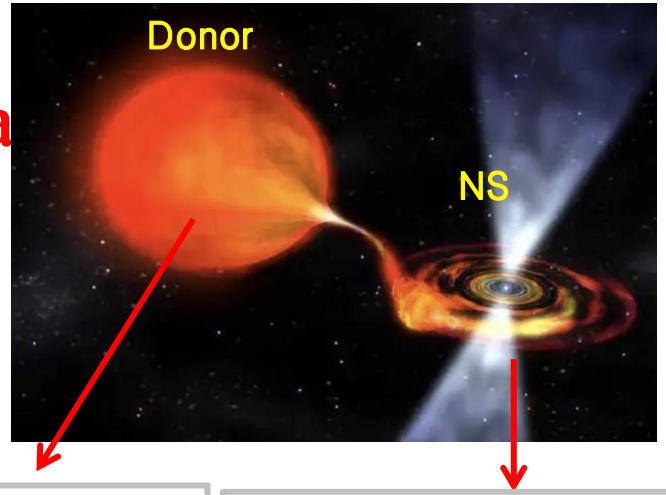

- Ultra-light companion stars (<0.1 $M_\odot$)
- Close orbit

  Have experienced mass-transfer

ultra-low M, short Porb:
Have transfer much material

high B, low spin:
Have not accrete material

✓AIC events is a possible solution!

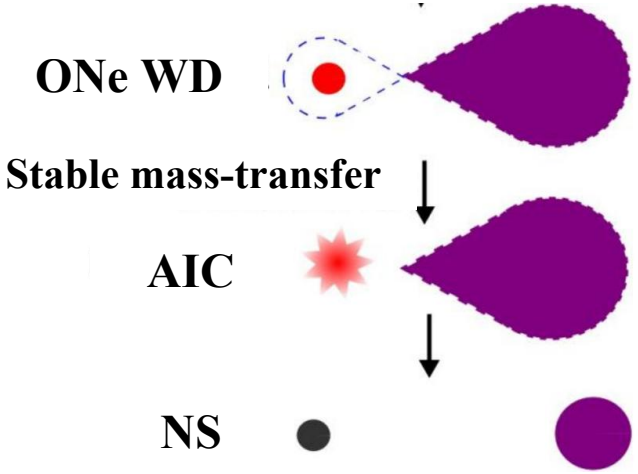

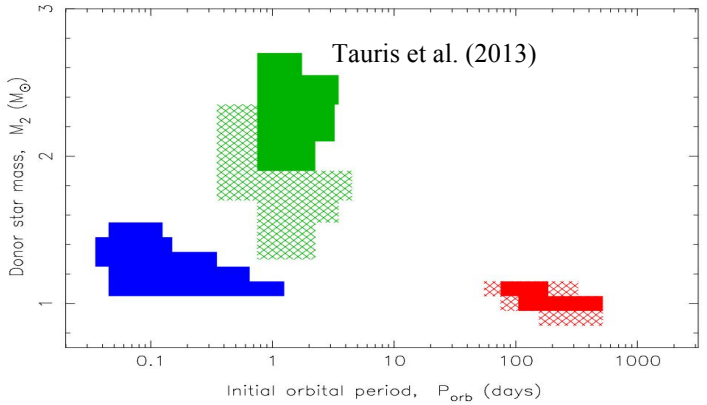

However, the donor mass after AIC is too large!

ONe WD+He WD systems to UCXBs Liu & Wang (2023)

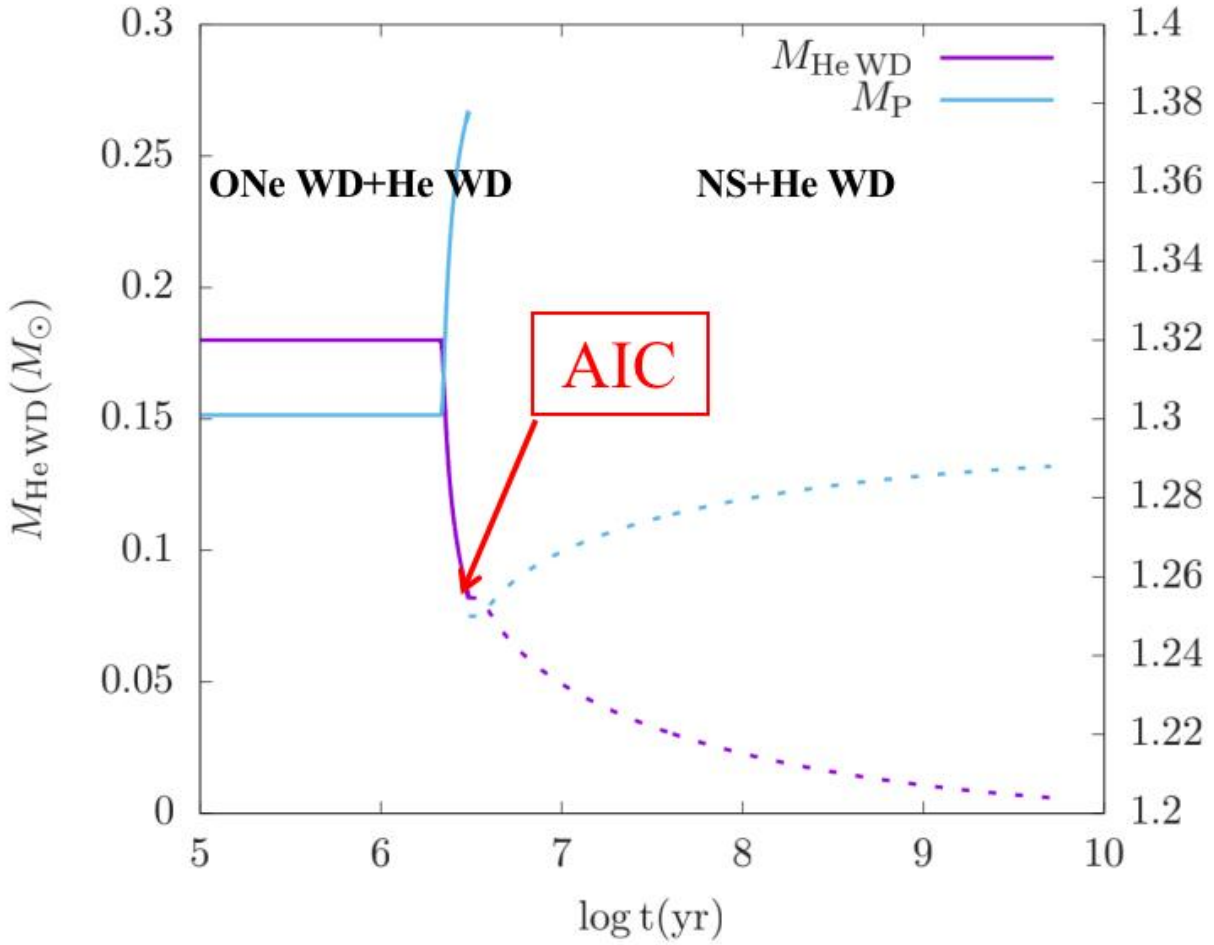

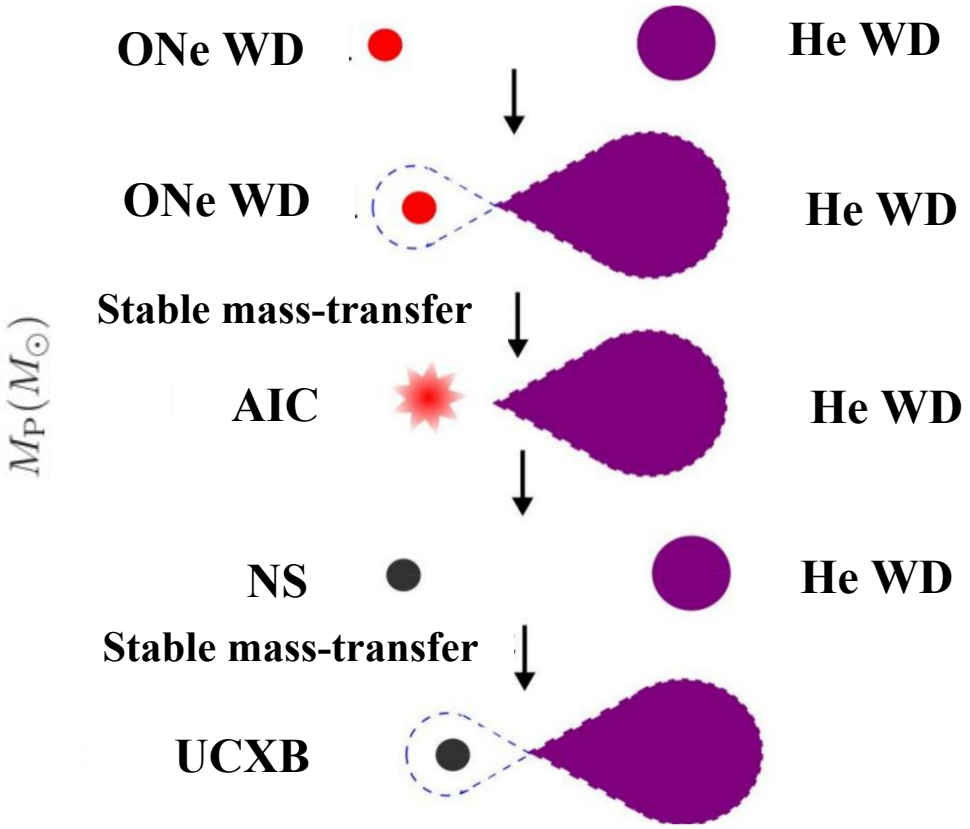

Reproducing 4U 1626-67

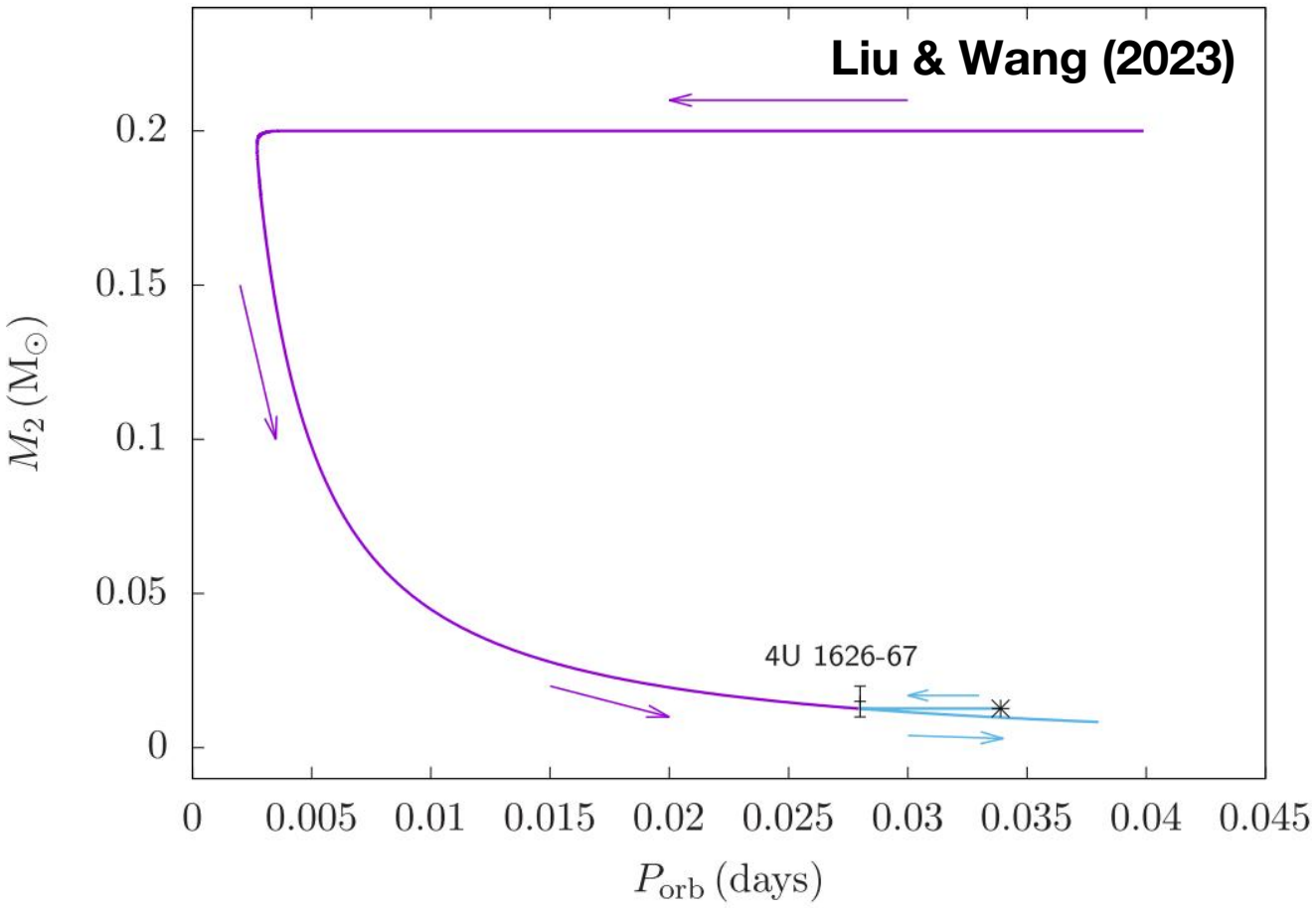

$M_{ONe\ WD}$= 1.26562 $M_\odot$; $M_{He\ WD}$=0.2 $M_\odot$; P_{orb}=0.045 d

Summary

The accretion-induce collapse of WDs can produce some particular NS systems:

1) ONe WD+MS channel: to MSPs with short orbital periods

2) ONe WD+RG channel: to MSPs with long orbital periods

3) ONe WD+He star channel: to IMBPs with short orbital periods

4) Double WD merger model: to isolated NSs

5) ONe WD+He WD channel: to UCXBs

Thanks for your attention!

liudongdong@ynao.ac.cn

Detections of AIC events I:

Radio light curves of AIC events from the SD model

Table 1
Predicted AIC Ejecta Properties

Model	M_{ej} $M_\odot$	E_{ej} 10^{51} erg	$M_{^{56}Ni}$ $M_\odot$	Reference
A	$\sim 10^{-3}$	~0.01	$\sim 10^{-4}$	Dessart et al. (2006)
B	~0.1	~1	$\sim 10^{-4}$	Dessart et al. (2007)
C	~0.01	~0.1	~0.01	Metzger et al. (2009)

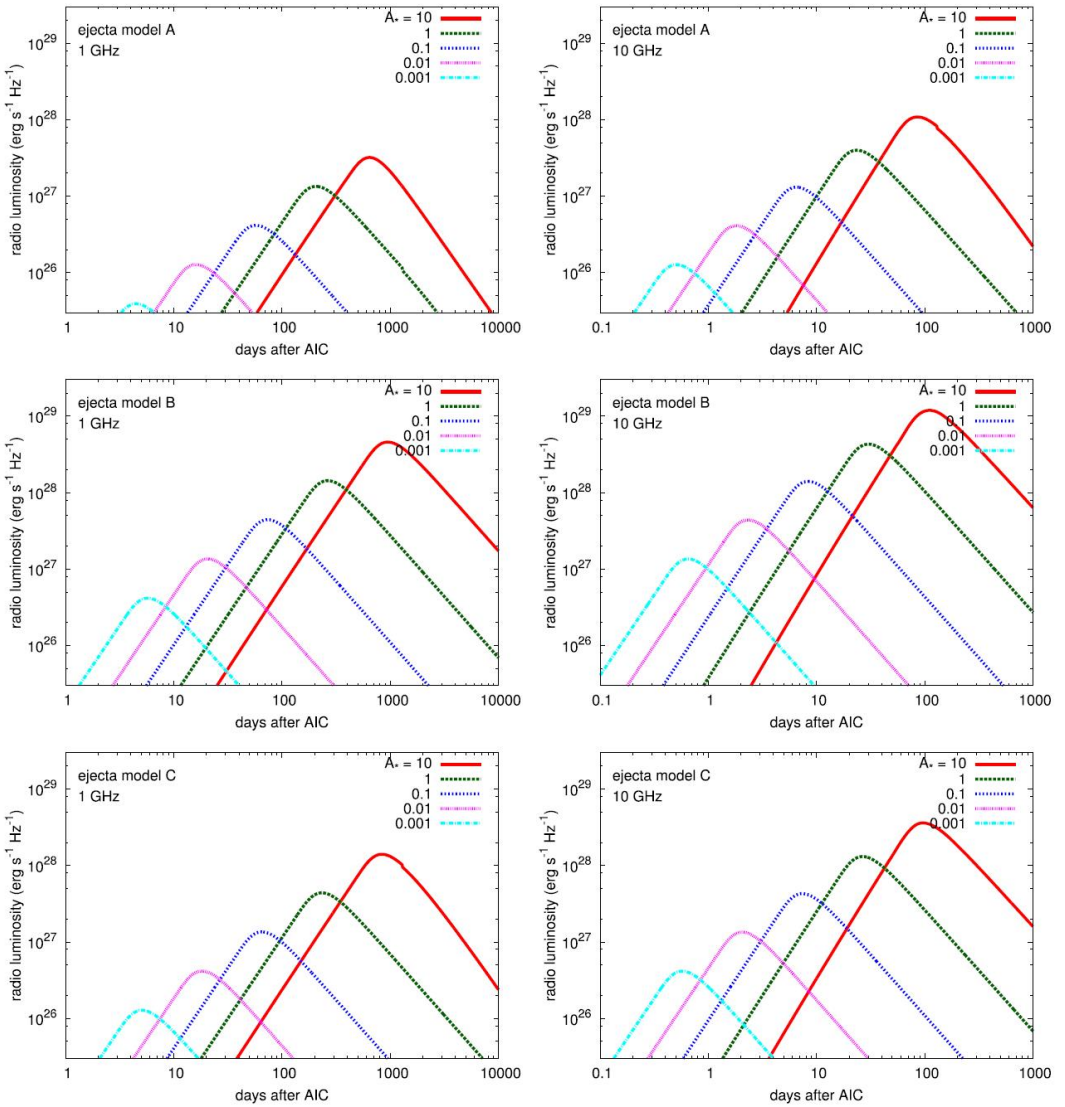

Figure 1. Radio LCs of AIC from SD systems at 1 and 10 GHz with the different ejecta properties (Table 1) and the different CSM densities ($A_* = 0.001$–10). Note the difference in the x axis in the right and left panels.

Moriya (2016)

Detectable for future space-based GW telescope

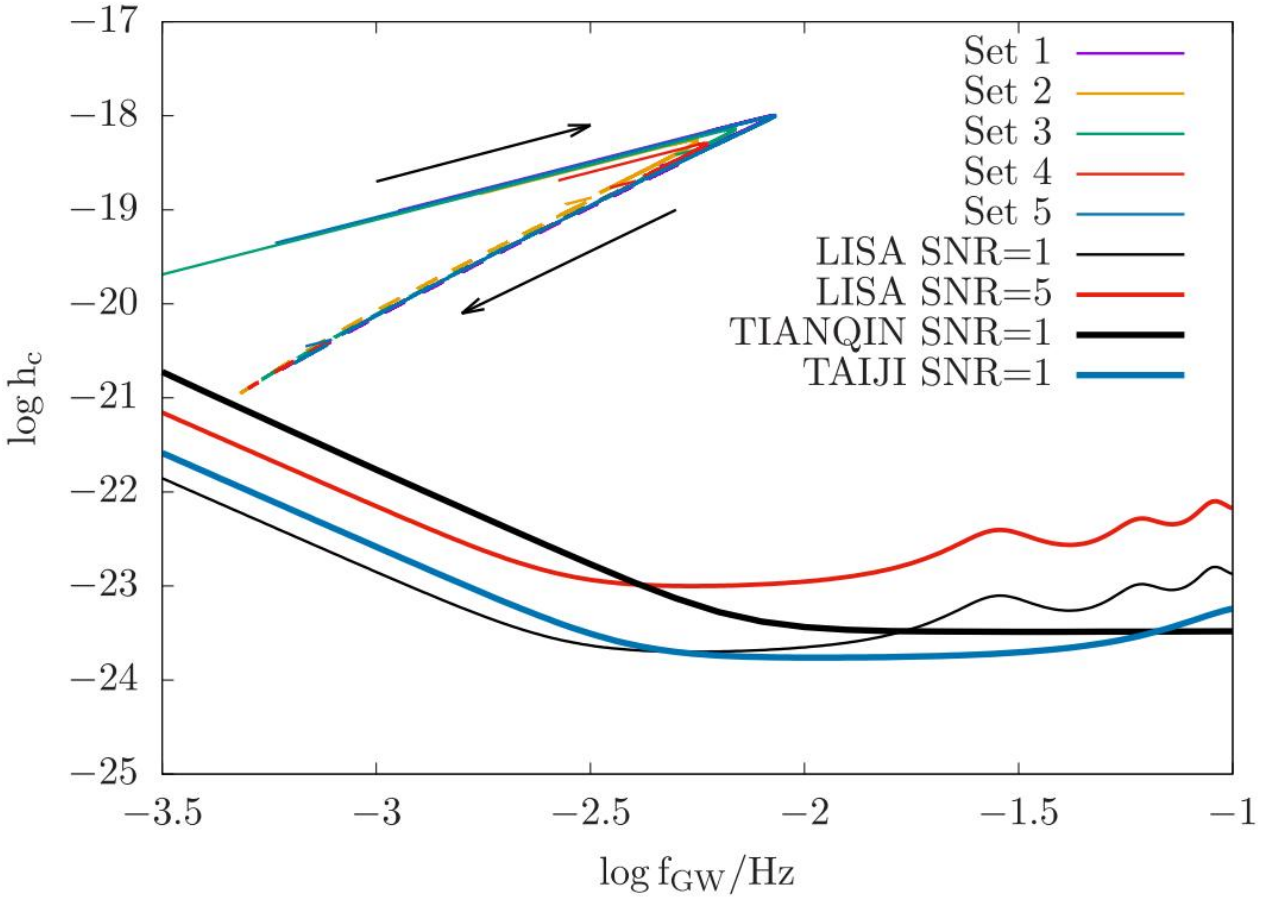

Liu & Wang (2023)

Set	$M^{\rm i}_{\rm ONe\,WD}$ ($M_\odot$)	$M^{\rm i}_2$ ($M_\odot$)	$P^{\rm i}_{\rm orb}$ (d)	δt_1 (Myr)	$M^{\rm AIC}_2$ ($M_\odot$)	$P^{\rm AIC}_{\rm orb}$ (d)	δt_2 (Gyr)	$M^{\rm f}_{\rm NS}$ ($M_\odot$)	$M^{\rm f}_2$ ($M_\odot$)	$P^{\rm f}_{\rm orb}$ (d)
1	1.3	0.2	0.015	0.21	0.1172	0.0051	1.65	1.3033	0.0082	0.0385
2	1.3	0.18	0.03	0.92	0.0819	0.0084	5.08	1.2880	0.0059	0.0481
3	1.34	0.18	0.08	0.11	0.1399	0.0046	4.13	1.3110	0.0062	0.0468
4	1.33	0.15	0.015	0.41	0.0933	0.0066	3.85	1.2935	0.0063	0.0461
5	1.26562	0.2	0.045	407.9	0.0127	0.0339	1.15	1.2522	0.0084	0.0380

ONe WD+He WD channel?

Mass-transfer process is dynamically stable

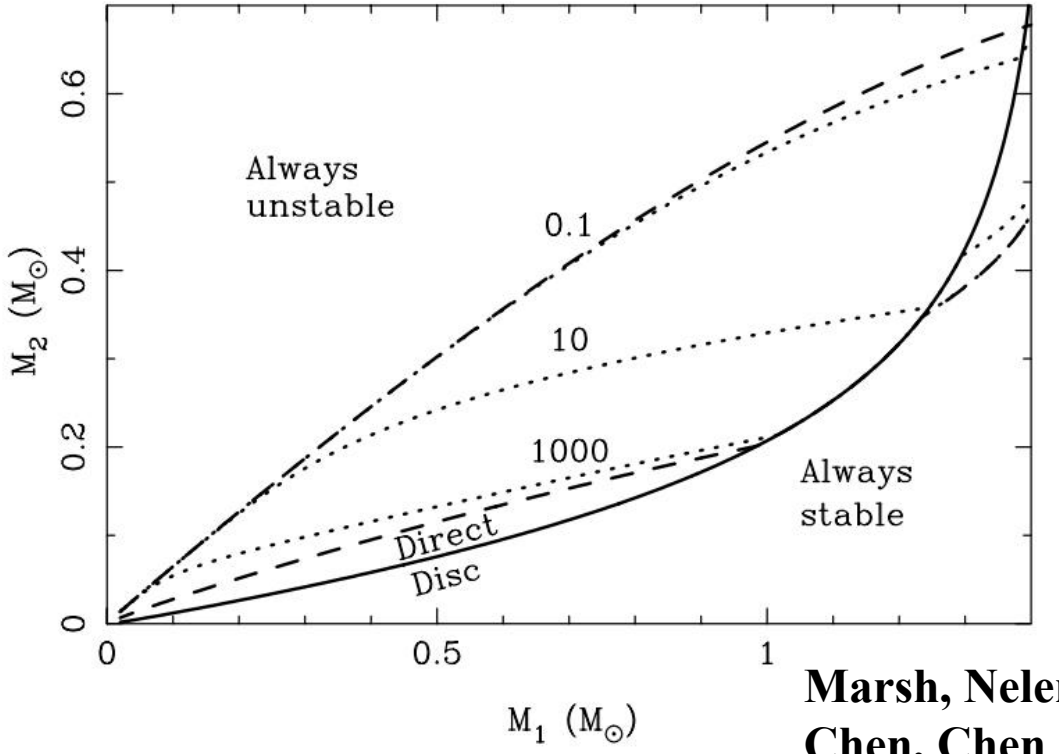

Marsh, Nelemans & Steeghs (2004)
Chen, Chen & Han(2022)

Figure 1. The upper dashed line shows the dynamical stability limit (equation 30), while the lower dashed line shows the stricter criterion of Nelemans et al. (2001) (equation 31), accounting for the switch between direct impact and disc accretion at $M_1 \approx 1\ M_\odot$. The solid line shows the transition between disc and direct impact accretion. The three dotted lines show how the strict stability limit of Nelemans et al. (2001) is relaxed when dissipative torques feed angular momentum from the accretor back to the orbit (equation 32), once again accounting for both the direct impact and disc accretion

An example

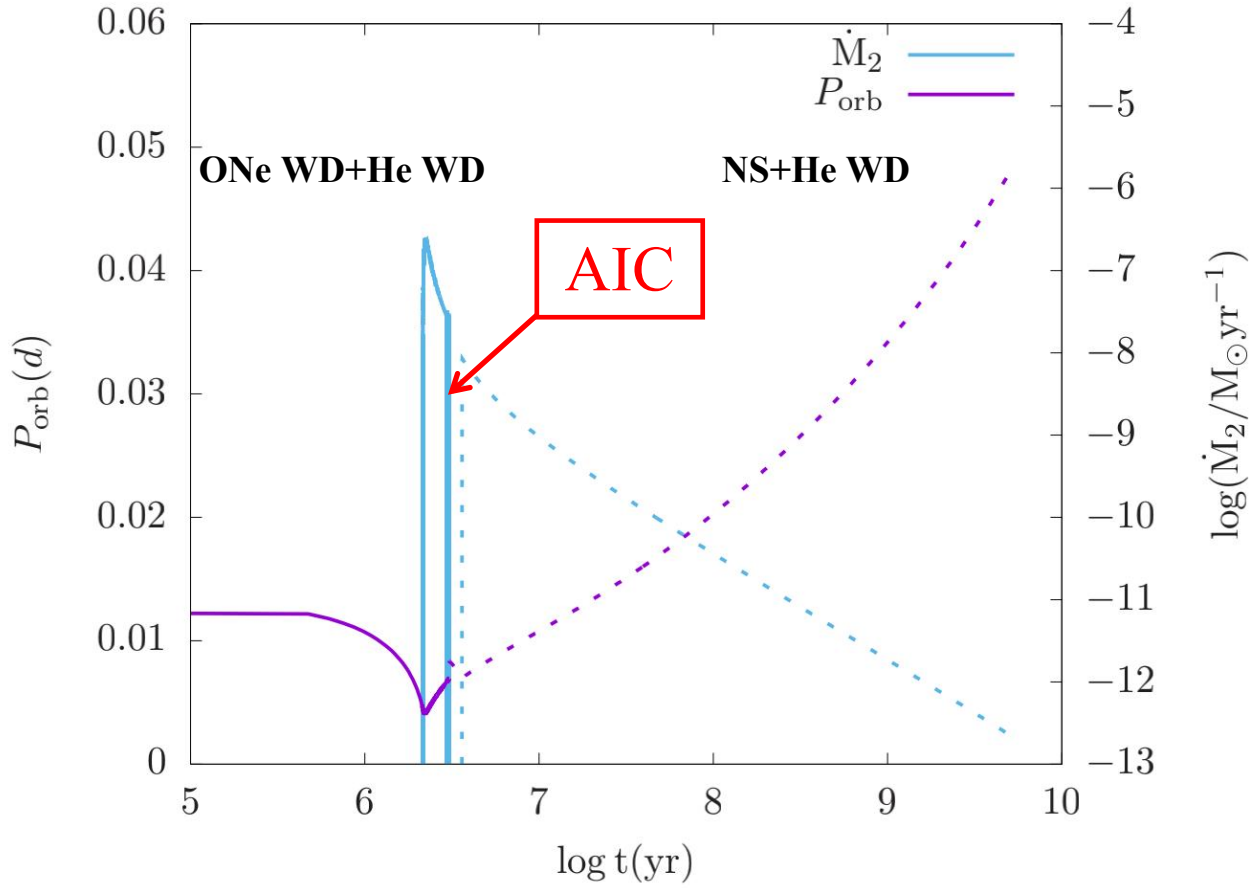

Liu, Wang+ (2022)

Mass-transfer rate—He WD mass

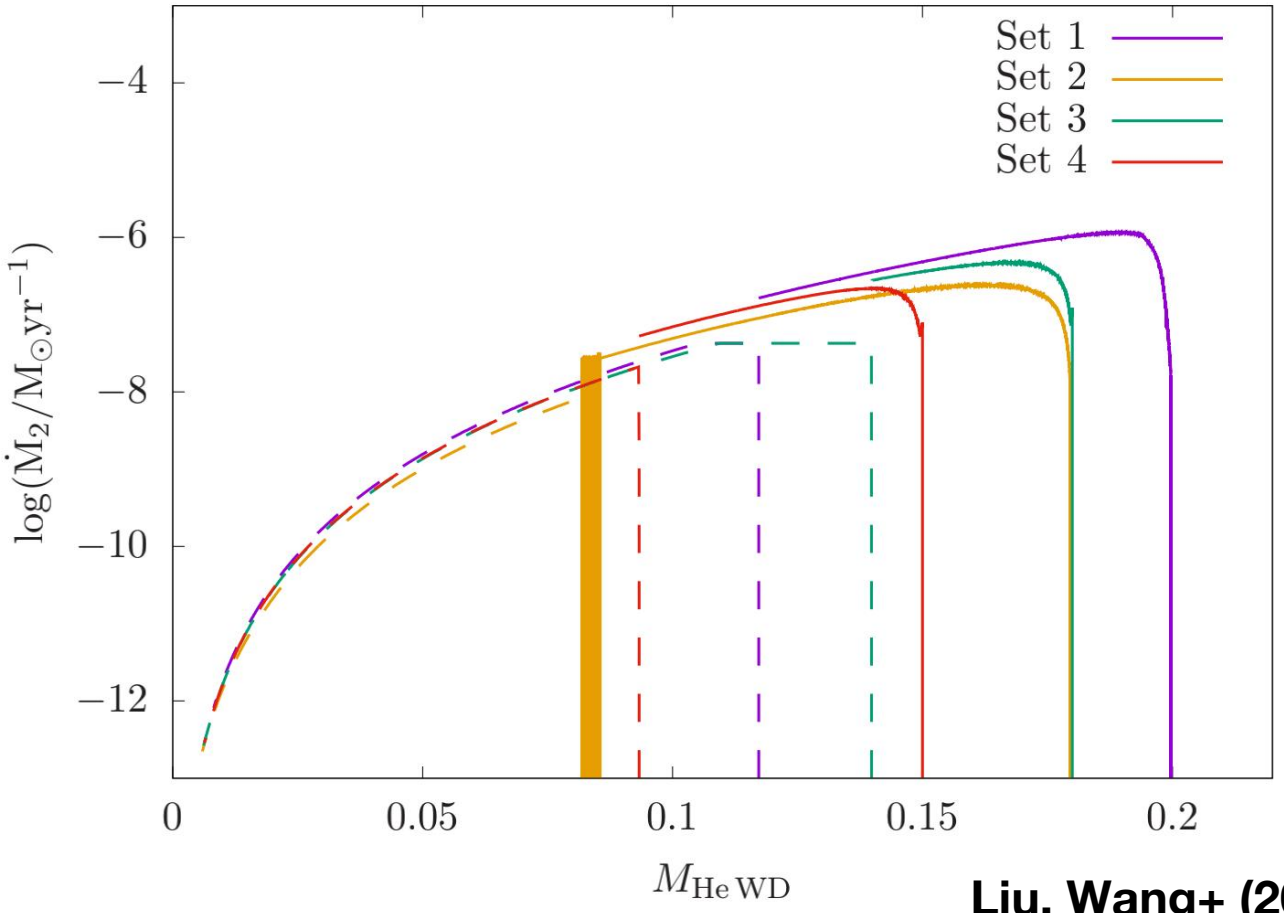

Liu, Wang+ (2022)

Detections of AIC events I: **VTC J095517.5+690813**

The SD model

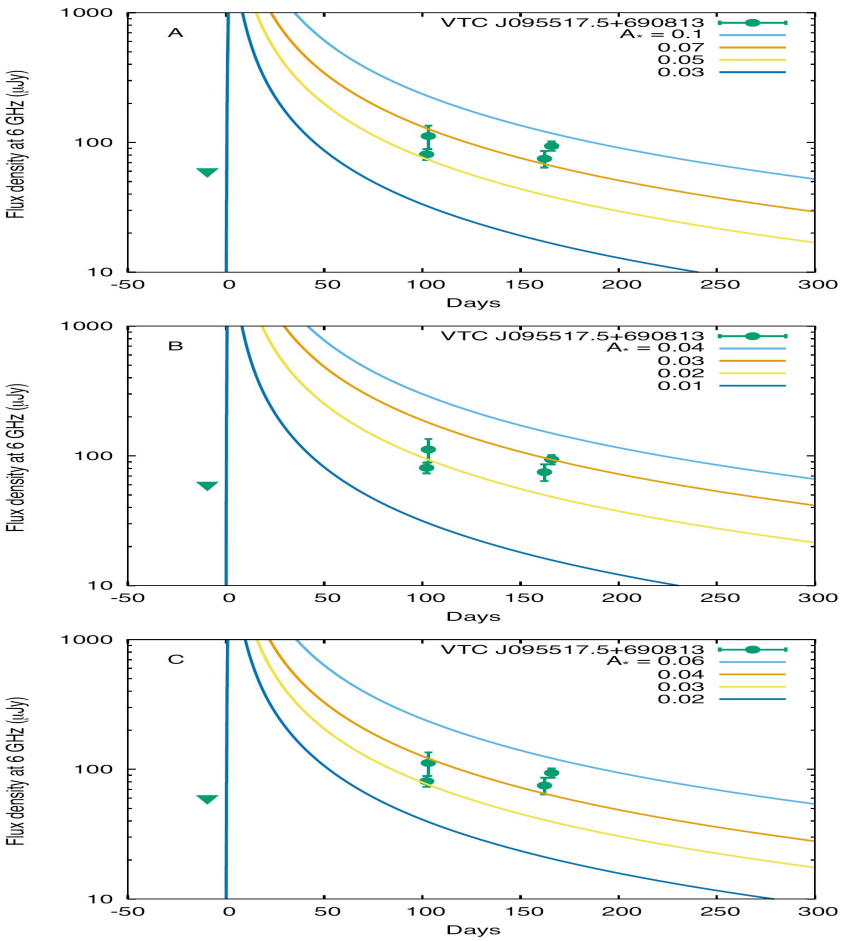

Figure 1. Radio (6 GHz) LC of AIC from the SD channel having the CSM density profile of $\rho_{\rm CSM}(r) = 5 \times 10^{11} A_* r^{-2}$ (cgs units) at the distance of VTC J095517.5 + 690813 (3.6 Mpc). The different panels have different ejecta properties (Table 1). The radio LC of VTC J095517.5 + 690813 at 6 GHz (Anderson et al. 2019) is presented for comparison. The triangle shows the upper flux limit. The explosion date of the synthetic LCs is 0 d, and the observed LC is shifted to compare with the synthetic LCs.

The DD model

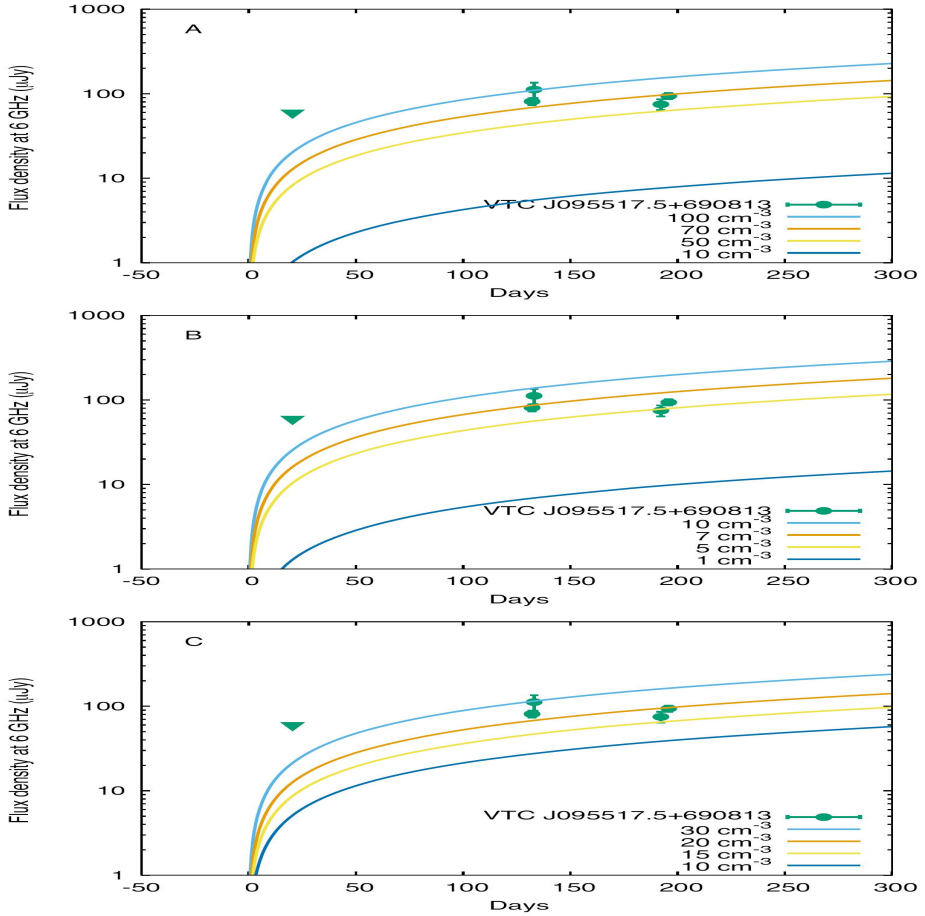

Figure 2. Radio (6 GHz) LC of AIC from the DD channel with a constant CSM density at the distance of VTC J095517.5 + 690813 (3.6 Mpc). The different panels have different ejecta properties (Table 1). The radio LC of VTC J095517.5 + 690813 at 6 GHz (Anderson et al. 2019) is presented for comparison. The triangle shows the upper flux limit. The explosion date of the synthetic LCs is 0 d, and the observed LC is shifted to compare with the synthetic LCs.

Moriya (2019)

双白矮星系统作为引力波信号源

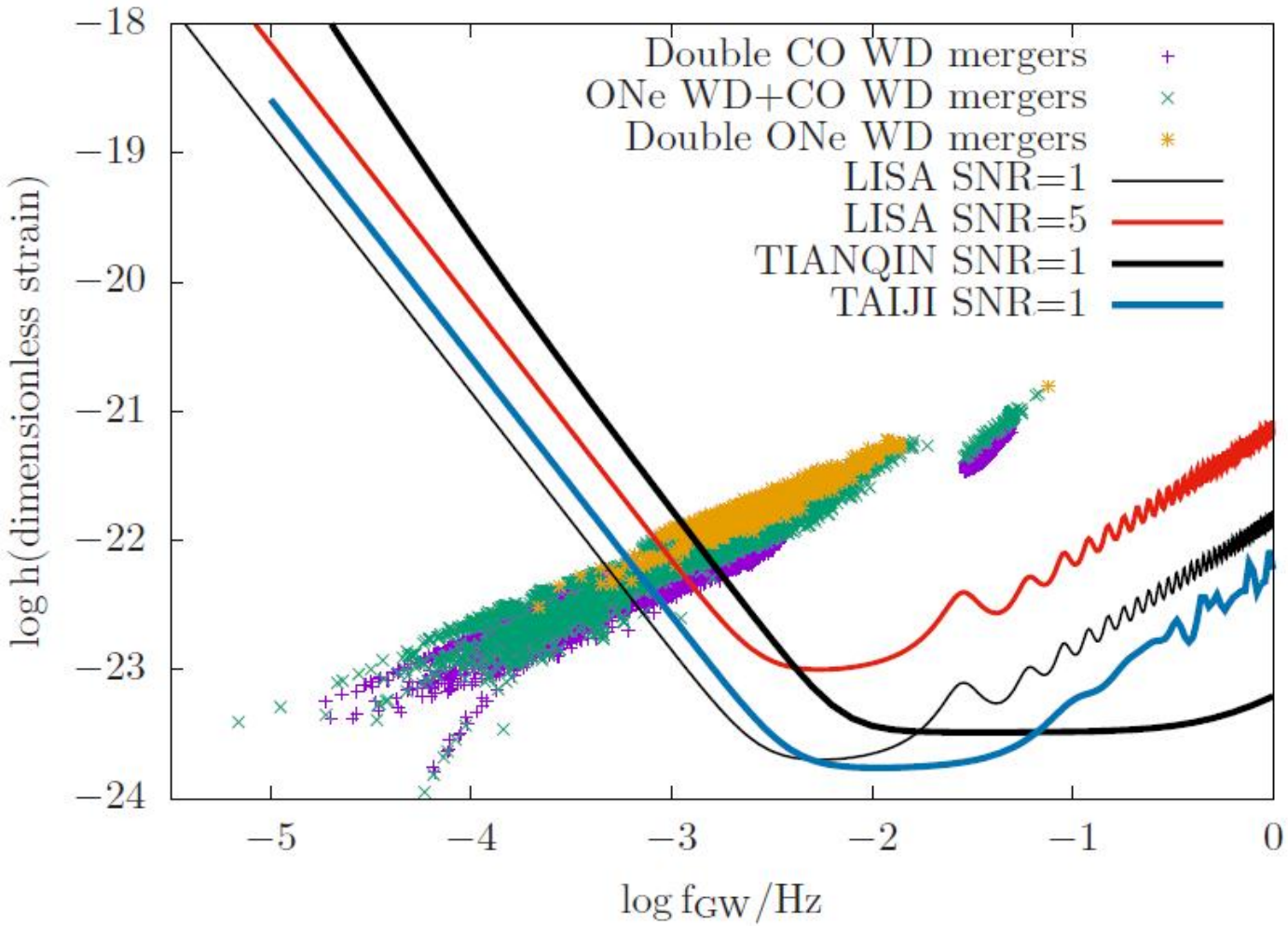

Liu & Wang, 2020, MNRAS, 494, 3422

Detections of AIC events II: **SN 2018kzr**

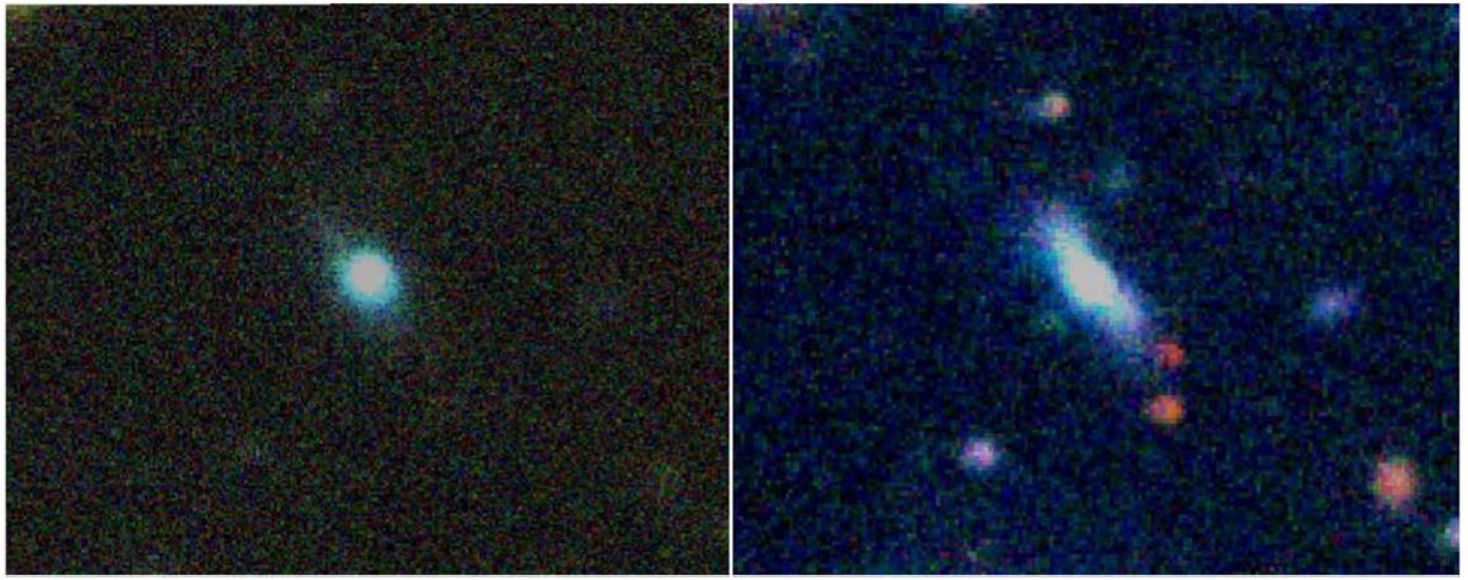

Figure 1. RGB composite images of the host of SN2018kzr, SDSS J082853.50+010638.6. Left: the GROND *gri* exposures from +3.731 days. Right: the NTT: EFOSC2 *gri* exposures taken at +68.676 days (Table 1). The host is a blue star-forming galaxy with a bright core.

The Second fastest declining supernova-like transient.

- ✓ **Peak magnitude: M_r=−17.98 (~1.4×10^{43} erg/s);**
- ✓ **Decline rate: 0.48±0.03 mag/day;**
- ✓ **Ejecta mass: M_{ej}=0.10±0.05Msun**

Mcbrien et al. (2019)

Detections of AIC events I: **VTC J095517.5+690813**

The SD model

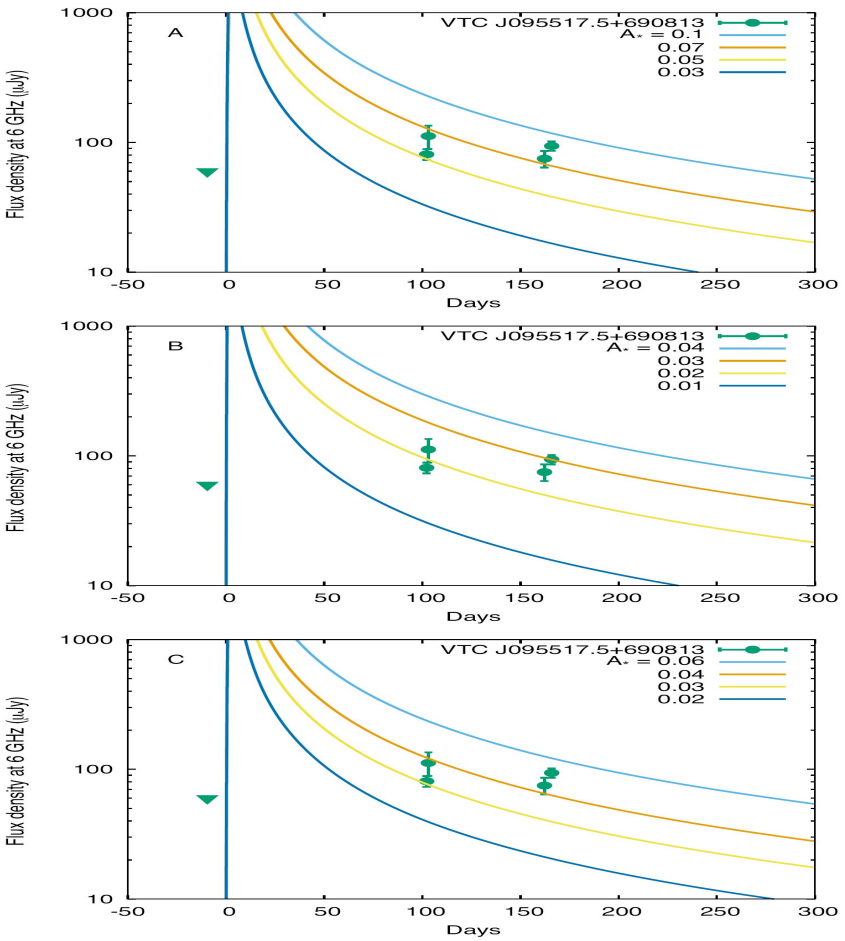

Figure 1. Radio (6 GHz) LC of AIC from the SD channel having the CSM density profile of $\rho_{\rm CSM}(r) = 5 \times 10^{11} A_* r^{-2}$ (cgs units) at the distance of VTC J095517.5 + 690813 (3.6 Mpc). The different panels have different ejecta properties (Table 1). The radio LC of VTC J095517.5 + 690813 at 6 GHz (Anderson et al. 2019) is presented for comparison. The triangle shows the upper flux limit. The explosion date of the synthetic LCs is 0 d, and the observed LC is shifted to compare with the synthetic LCs.

The DD model

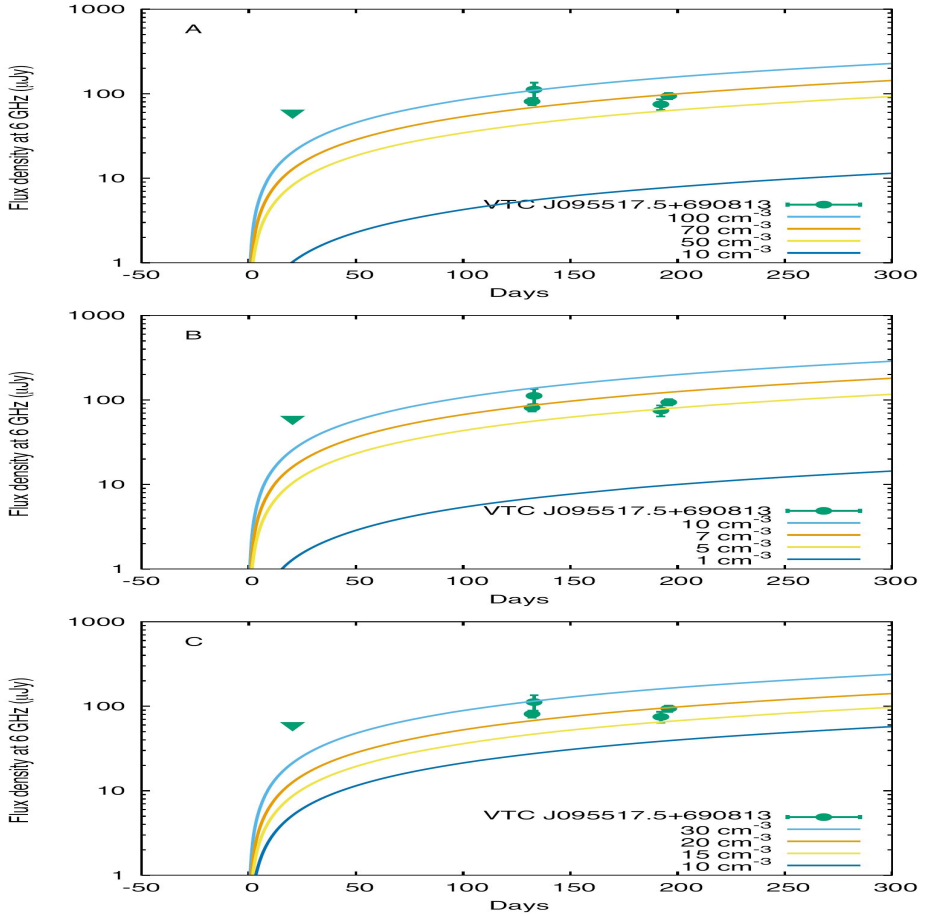

Figure 2. Radio (6 GHz) LC of AIC from the DD channel with a constant CSM density at the distance of VTC J095517.5 + 690813 (3.6 Mpc). The different panels have different ejecta properties (Table 1). The radio LC of VTC J095517.5 + 690813 at 6 GHz (Anderson et al. 2019) is presented for comparison. The triangle shows the upper flux limit. The explosion date of the synthetic LCs is 0 d, and the observed LC is shifted to compare with the synthetic LCs.

Moriya (2019)

Yu Yunwei

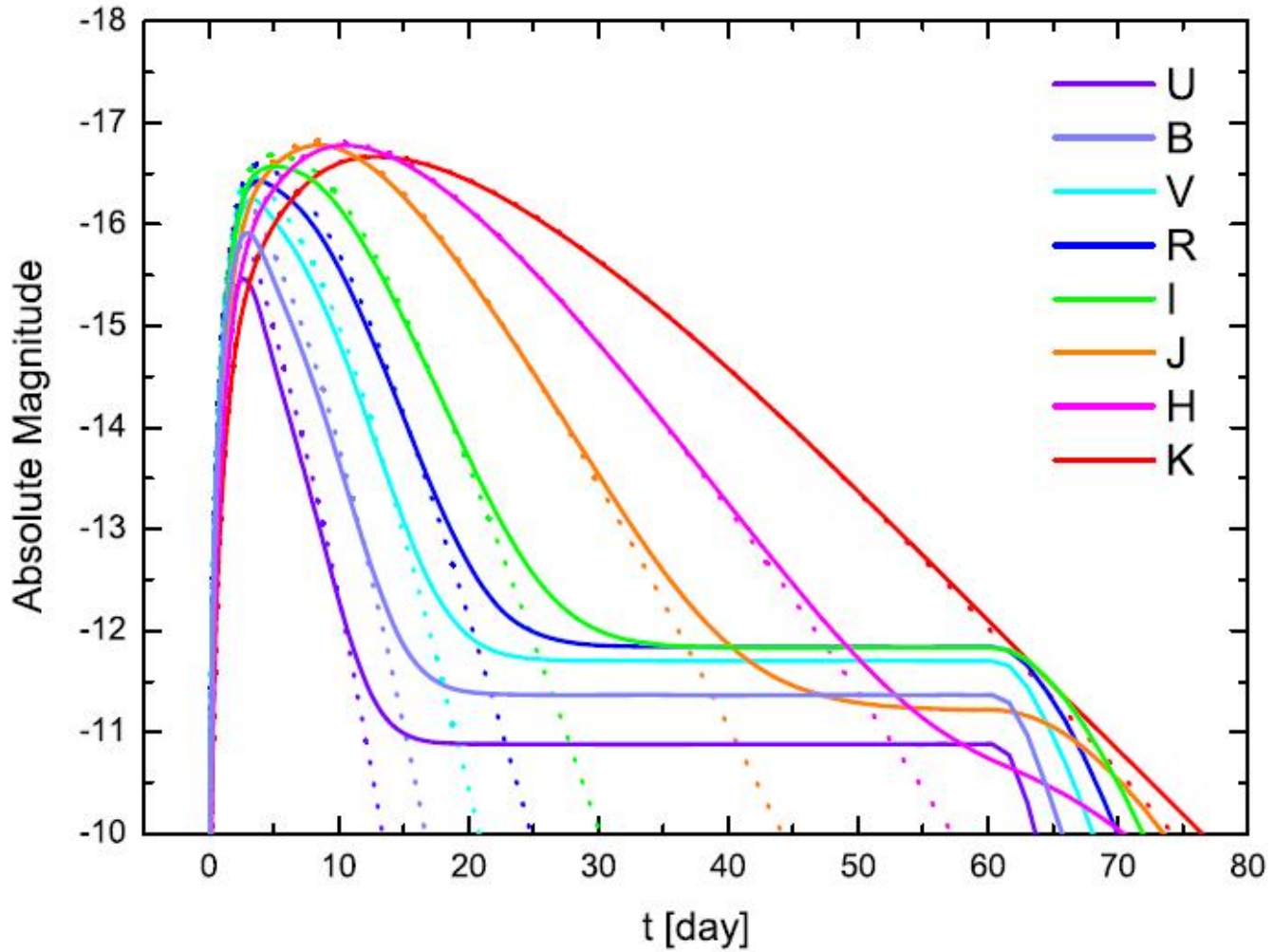

Figure 3. Multiband light curves affected (solid lines) and unaffected (dotted lines) by a dusty wind shell.

轨道周期在几十至几百天的毫秒脉冲星的形成？

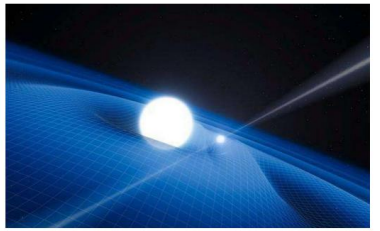

脉冲星+白矮星

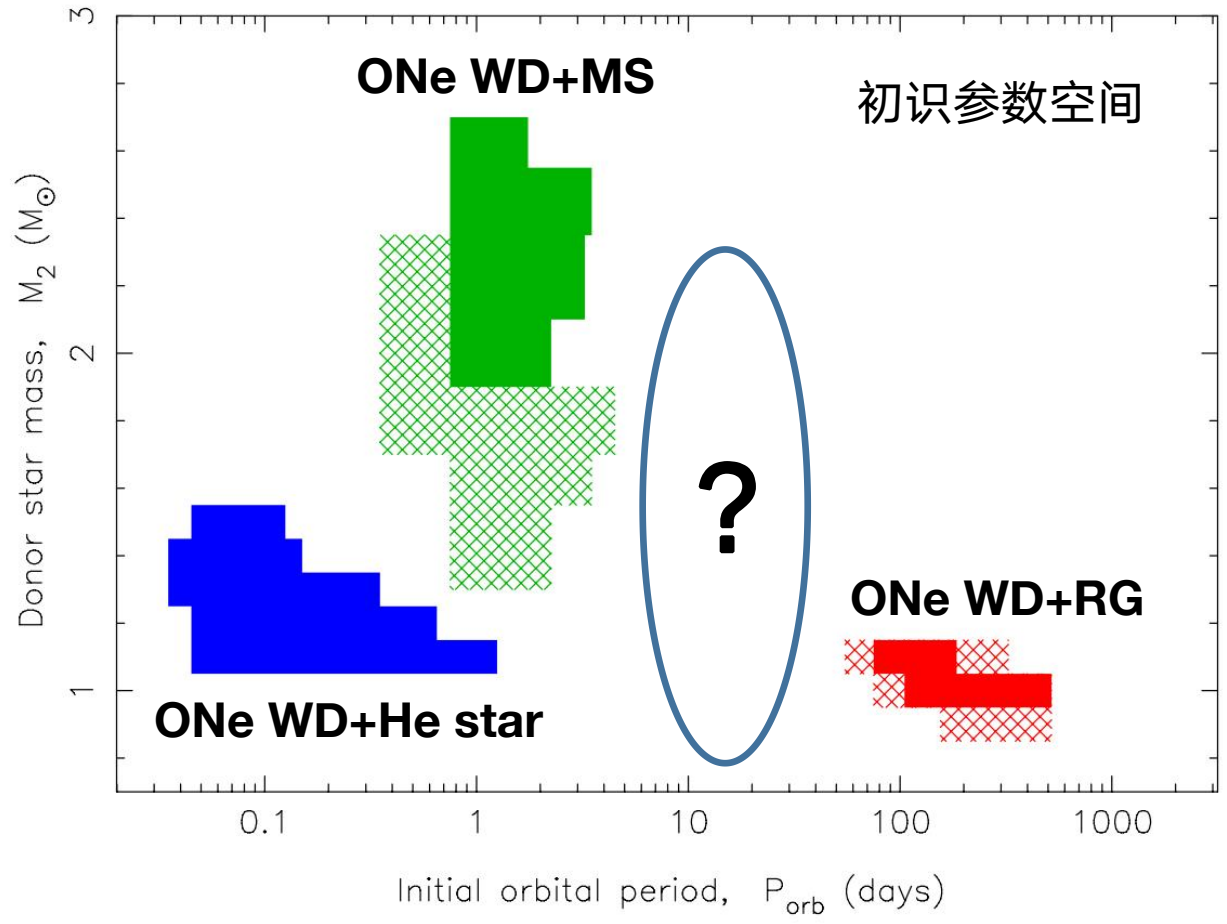

Tauris et al. (2013)

原因分析：RLOF的物理机制

Previous models:

$$\dot{M}_2 = -C\max[0,(\frac{r_{star}}{r_{lobe}} - 1)^3],$$

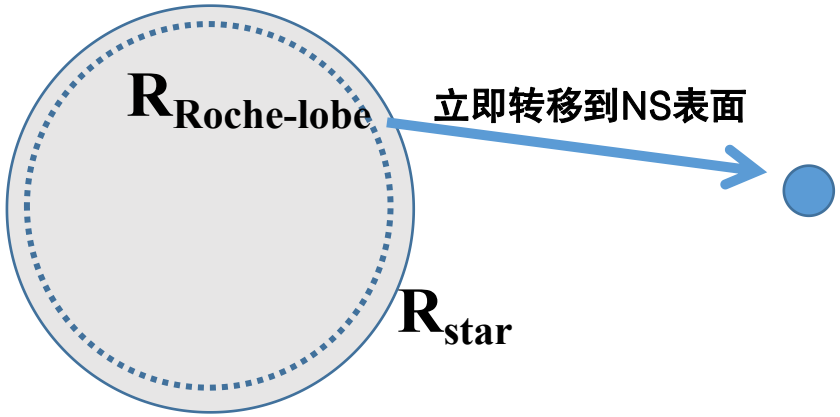

The exceeding mass of the donor would be transferred onto WD immediately as soon as the donor star exceeds its Roche-lobe.

In this case, the mass-transfer rate is usually relatively high, resulting in two cases that prevent the formation of SNe Ia: (1) common envelope phase;

(2) Stronge stellar wind phase.

更适合主序星伴星的情况

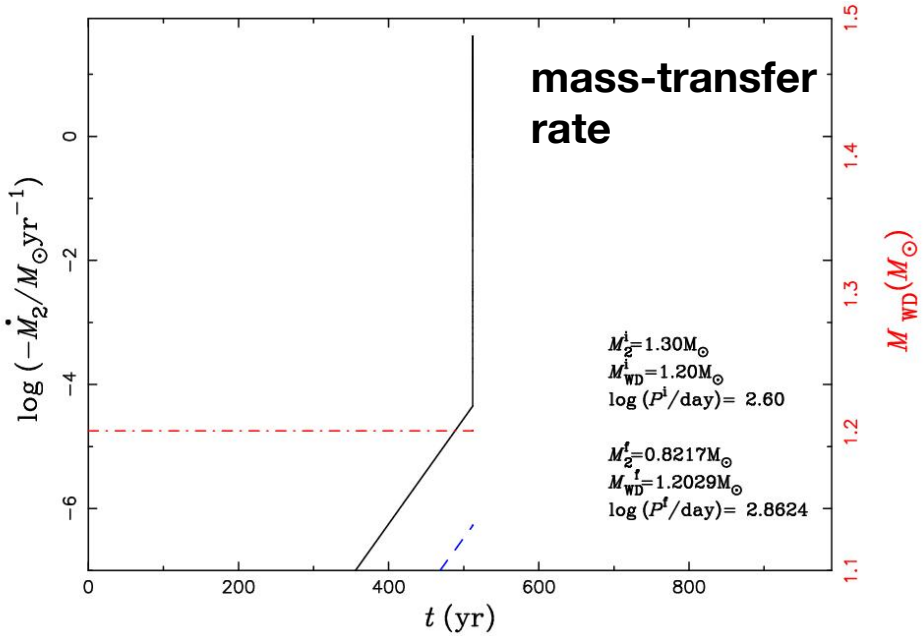

Improved the mass-transfer prescription:

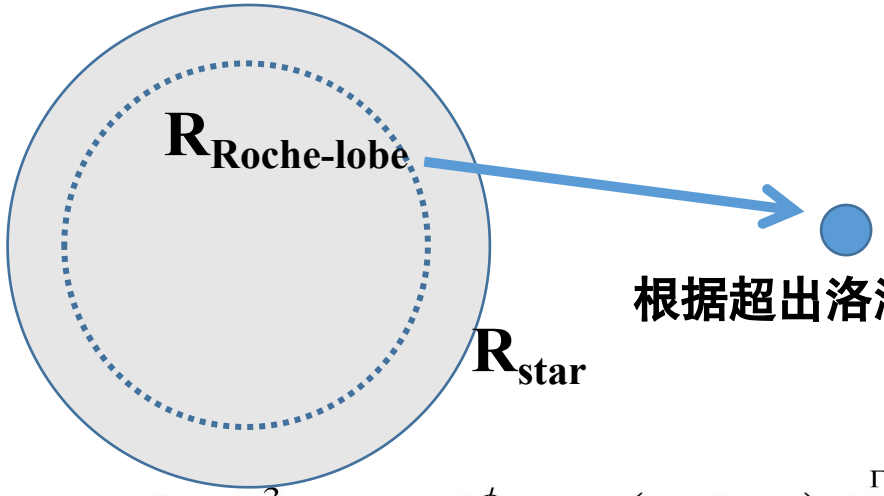

根据超出洛溪瓣部分的物态计算质量转移率，
适用范围更广

$$\dot{M}_1 = -\frac{2\pi R_L^3}{GM_1} f(q) \int_{\phi_L}^{\phi_s} \Gamma_1^{\frac{1}{2}} \left(\frac{2}{\Gamma_1+1}\right)^{\frac{\Gamma_1+1}{2(\Gamma_1-1)}} (\rho P)^{\frac{1}{2}} d\phi, \tag{A9}$$

where ϕ_s is the stellar surface potential, and we have used the relation $R_{\rm L} = r_{\rm L} A$. We have combined factors dependent on the mass ratio in the coefficient

$$f(q) \equiv \frac{q}{r_{\rm L}^3(1+q)} \frac{1}{[a_2(a_2-1)]^{1/2}}, \tag{A10}$$

a slowly-varying function of q. For the integration over potential ϕ, we use the approximation

Ge et al. 2010

AIC events
from ONe WD+ONe/CO WD mergers

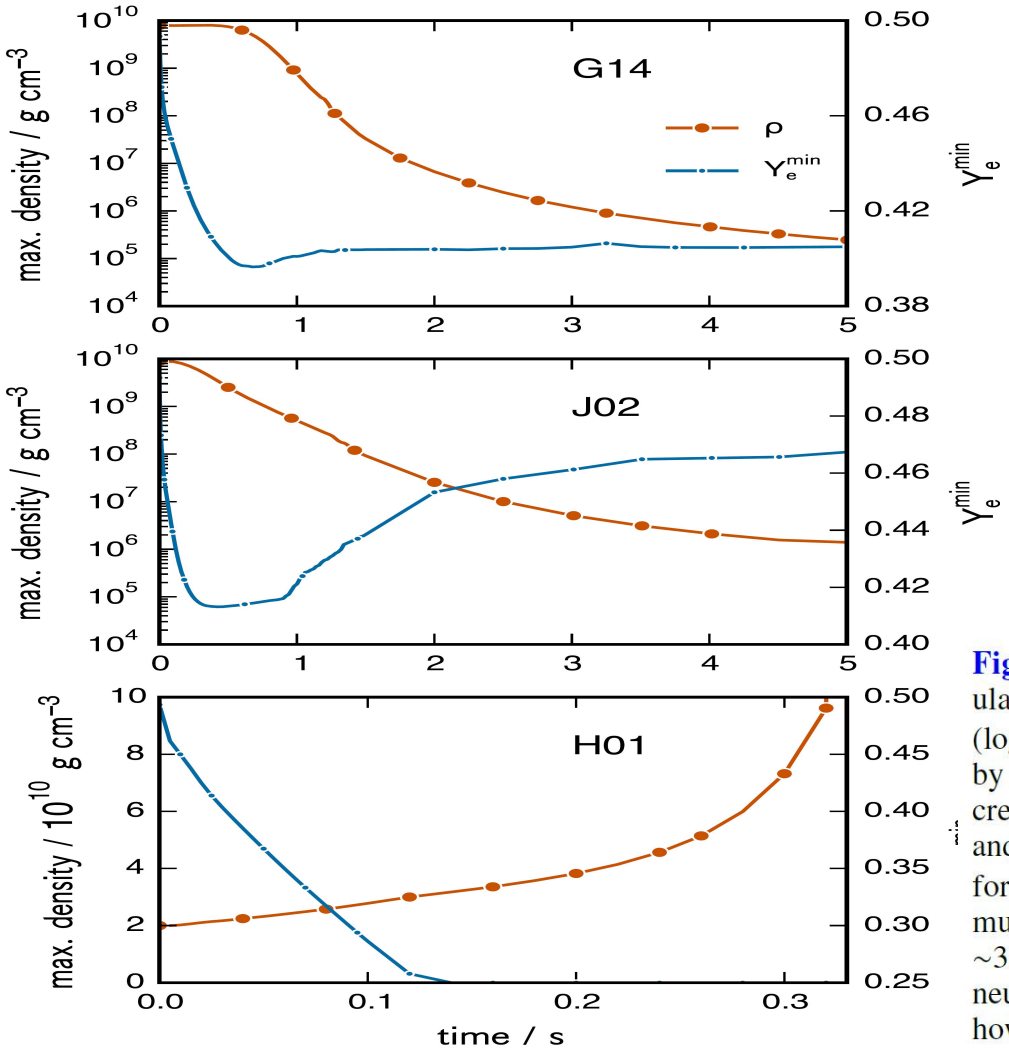

Jones et al. (2016)

First multidimensional hydrodynamic simulations of the oxygen deflagration

Fig. 2. Maximum density and minimum electron fraction Y_e in the simulations G14, J02 and H01 (see Table 1). In the G and J simulations ($\log_{10}\rho_c^{ign}$ = 9.9 and 9.95), respectively, the maximum density drops by several orders of magnitude in the first 5 s despite the marked decrease in the minimum Y_e, leading to the partial disruption of the core and the formation of an ONeFe white dwarf that does not collapse to form a neutron star. In the H01 simulation ($\log_{10}\rho_c^{ign}$ = 10.3), the maximum density only increases with time, reaching 10^{11} g cm^{-3} in the first ~330 ms. The simulation was not continued beyond this point because neutrino interactions with matter were not included in the microphysics, however the most likely outcome is collapse into a neutron star.